

**GRAPHENE TEXTILE SMART CLOTHING FOR WEARABLE
CARDIAC MONITORING**

by
GİZEM ACAR

Submitted to the Graduate School of Engineering and Natural Sciences
in partial fulfilment of
the requirements for the degree of Master of Science

Sabancı University
December 2019

**GRAPHENE TEXTILE SMART CLOTHING FOR WEARABLE
CARDIAC MONITORING**

Approved by:

Asst. Prof. Dr. Murat Kaya YAPICI
(Thesis Supervisor)


.....

Asst. Prof. Dr. Serap HAYAT SOYTAŞ


.....

Prof. Dr. Arda Deniz YALÇINKAYA


.....

Approval Date: December 9, 2019

GİZEM ACAR 2019 ©

All Rights Reserved

ABSTRACT

GRAPHENE TEXTILE SMART CLOTHING FOR WEARABLE CARDIAC MONITORING

GİZEM ACAR

ELECTRONICS ENGINEERING M.Sc. THESIS, ARALIK 2019

Thesis Supervisor: Asst. Prof. Dr. Murat Kaya Yapıcı

Keywords: wearable electronics; graphene; textile; ECG; IoT; m-health; e-textile; biopotential; electrode; health monitoring; flexible, stencil printing, dip coating

Wearable electronics is a rapidly growing field that recently started to introduce successful commercial products into the consumer electronics market. Employment of biopotential signals in wearable systems as either biofeedbacks or control commands are expected to revolutionize many technologies including point of care health monitoring systems, rehabilitation devices, human–computer/machine interfaces (HCI/HMIs), and brain–computer interfaces (BCIs). Since electrodes are regarded as a decisive part of such products, they have been studied for almost a decade now, resulting in the emergence of textile electrodes. This study reports on the synthesis and application of graphene nanotextiles for the development of wearable electrocardiography (ECG) sensors for personalized health monitoring applications. In this study, we show for the first time that the electrocardiogram was successfully obtained with graphene textiles placed on a single arm. The use of only one elastic armband, and an “all-textile-approach” facilitates seamless heart monitoring with maximum comfort to the wearer. The functionality of

graphene textiles produced using dip coating and stencil printing techniques has been demonstrated by the non-invasive measurement of ECG signals, up to 98% excellent correlation with conventional pre-gelled, wet, silver/silver-chloride (Ag / AgCl) electrodes. Heart rate have been successfully determined with ECG signals obtained in different situations. The system-level integration and holistic design approach presented here will be effective for developing the latest technology in wearable heart monitoring devices.

ÖZET

GIYİLEBİLİR KARDİYOVASKÜLER TAKİP İÇİN GRAFEN TEKSTİL TABANLI AKILLI GIYSİ

GİZEM ACAR

ELEKTRONİK MÜHENDİSLİĞİ YÜKSEK LİSANS TEZİ, ARALIK 2019

Tez Danışmanı: Dr. Öğr. Üyesi Murat Kaya Yapıcı

Anahtar Kelimeler: giyilebilir elektronikler; grafen; Tekstil; EKG; IOT, HCI; E-tekstil; biyopotansiyel; elektrot; sağlık izleme; esnek, şablon baskı, daldırma kaplama

Giyilebilir elektronik, son zamanlarda tüketici elektroniği pazarına başarılı ticari ürünler sunmaya başlayan hızla büyüyen bir alandır. Biyogeribildirim veya kontrol komutları gibi giyilebilir sistemlerde biyopotansiyel sinyallerin istihdam edilmesinin, bakım noktası sağlık izleme sistemleri, rehabilitasyon cihazları, insan-bilgisayar / makine arayüzleri (HCI / HMI'ler) ve beyin-bilgisayar arayüzleri (BCI'ler) dahil olmak üzere birçok teknolojiye devrim yaratması beklenmektedir. Elektrotlar bu tür ürünlerin belirleyici bir parçası olarak görüldüğünden, neredeyse on yıldır incelenmiş ve tekstil elektrotlarının ortaya çıkmasına neden olmuştur. Bu çalışma, kişiselleştirilmiş sağlık izleme uygulamaları için giyilebilir elektrokardiyografi (EKG) sensörlerinin geliştirilmesi için grafen nanotekstillerin sentezi ve uygulaması hakkında rapor vermektedir. Bu çalışmada ilk kez elektrokardiyogramın tek bir kola yerleştirilen grafen tekstillerle başarılı bir şekilde elde edildiğini gösterdik. Sadece bir elastik kol bandı ve “tüm tekstil yaklaşımı” kullanımı, kullanıcının kesintisiz kalp izleme sağlamasını kolaylaştırır. Daldırma kaplama ve şablon baskı teknikleri kullanılarak üretilen grafen tekstillerinin işlevselliği,

EKG sinyallerinin invaziv olmayan ölçümü, geleneksel ön jelleşmiş, ıslak, gümüş / gümüş-klorür (Ag / AgCl) ile grafen elektrotlar karşılaştırıldığında % 98'e kadar mükemmel korelasyon ile gösterilmiştir. Farklı durumlarda güçlü bir şekilde elde edilen EKG sinyalleriyle kalp atış hızı oranları başarıyla belirlenmiştir. Burada sunulan sistem düzeyinde entegrasyon ve bütünsel tasarım yaklaşımı, giyilebilir kalp izleme cihazlarında en son teknolojinin geliştirilmesinde etkili olacaktır.

ACKNOWLEDGEMENTS

I would like to express my sincere appreciation to Professor Murat Kaya Yapıcı, a great supervisor: He guided me persuasively even when the road became difficult and encouraged me to be professional and do the right thing. I am grateful him for sharing the time to listen to me whenever I have any problems, that have allowed me to improve myself in every way, for assisting in his lessons and for his excellent guidance. I would like to thank him endlessly for his trust and support in making me a family member of SU-MEMS.

The most undesirable part to take courses at the Master is perhaps the courses taken outside the department. This was not the case for me thanks to Professor Ali Koşar. I would like to thank him, who was honored to take his course and to enroll projects together, for supporting me and sharing his ideas with me.

In addition, I thank to Professor Enver Bulur and Professor Hande Toffoli very much. Even though I graduated from METU, they do not stint their support as guidance.

During the period, I have learned a lot about life and academics at Sabancı University and I had great memories. I am appreciated my teammate Osman Şahin for the time we have spent together for which the food he cooked and everything he helped, since i began to Sabanci university. Even if you forget your cell phone occasionally, I hope you don't forget those memories. 😊

Also, I would like to thank other my teammate Özberk Öztürk, who I enjoyed working with in the same project group and who led me to experience enlightenment from time to time. Also I am grateful to his USB to storage our all data 😊 I would also like to thank Farid Irani, Melih Can Taşdelen, Muhammet Genç, Rayan Bajwa, Ata Golparvar, Tuğçe Delipınar, Heba Ahmed Saleh, Ali Kasal and Sercan Tanyeli who are a member of the SU-MEMS family and is more of a family than a group and had helped me to work as a participant in my project.

I am also grateful to Metehan Can, Özgün Forlar, Sema Yıldırım and Oğuz Çetinkaya who volunteered to contribute the progress of my project even though they weren't in Istanbul. They have helped me every day and night whenever I needed them. Love you guys 😊

If you live in a dorm, one of the most important things is who your roommate is. I would like to thank my roommate Liyne Noğay for all the memories and good times she shared with me for 2 years.

I'm really appreciated to meet my friends Naz Ayvaz, Can Çalışkan, Abdul Rahman Dabbour and Emirhan Tümen who made this school more livable and bearable to me. And I would like to thank Zeki Semih Pehlivan who came running whenever I needed him for any help. He has made me understand even the issues that I didn't understand in the most obvious way.

I am also grateful to Özlem Karahan, who is so special as much as my sister. She has impressed me with her intelligence and support by being with me in my bad and good times. I am really thanking to her for listening to me indefinitely and for all our time.

And what I write for Rıdvan Ergun, my best birthday present in life, will not be enough to express my gratitude and love for him. I thank him forever for never leaving me alone, for his eternal love, support and happiness. So glad that I have you.

Finally, I must express my very profound gratitude to my parents Hatice and Şahin Acar and to my brother Erkut Acar for providing me with unfailing support and continuous encouragement throughout my years of study and through the process of researching and writing this thesis. This accomplishment would not have been possible without them.

Thank you again forever. I feel eternal pride and gratitude for being in my life.

*Dedicated to my grandparents
Cemile and Osman ACAR,
yearningly...*

Table of Contents

1. INTRODUCTION AND MOTIVATION.....	1
1.1. Introduction.....	1
1.2. Related Work	3
1.3. Summary of Work.....	5
1.4. Outline.....	6
2. BACKGROUND ON ELECTROCARDIOGRAM.....	8
2.1. Electrical Activity of Heart	8
2.2. ECG Signal Measurement and Lead Points	12
3. ELECTRODES FOR ELECTROCARDIOGRAM	16
3.1. Conventional Electrodes	16
3.2. Dry Electrodes.....	19
3.2.1. Contact Electrodes	19
3.2.2. Non-contact Electrodes	20
3.3. Textile Electrodes	22
3.3.1. Performance Characteristics	22
3.3.2. Materials and Methods.....	27
4. PREPARATION OF GRAPHENE COATED TEXTILE AND GRAPHENE ARMBAND	38
4.1. Textile Synthesis.....	38
4.2. Direct Patterning of Garments by Spray/Stencil Printing.....	42
4.3. ECG Acquisition Circuitry.....	44
4.4. Wearable Prototype.....	47
4.5. Skin Electrode Impedance	49

5. RESULTS AND DISCUSSION.....	51
5.1. Single Arm Band with Graphene Electrode.....	51
5.2. Graphene Garment	57
6. CONCLUSION AND FUTURE WORK.....	61
BIBLIOGRAPHY	64

LIST OF TABLES

Table 1.1 Summary of the various integrated textile system solutions categorized based on the acquired biopotentials to show the different manufacturing techniques and conductive materials used in their realization and the active sensing regions on the body.....	3
Table 4. 1 Component sections and specifications for signal acquisition system	47
Table 5. 1 Correlation Coefficients Between Signals Obtained with Graphene Textile And Ag/AgCl Electrodes	55
Table 5.2 Beat Per Minute (Bpm) Values For Eight Participants When Sitting, Standing And Walking.....	56

LIST OF FIGURES

Figure 1. 1 Wearable electrocardiography (ECG) systems: (a) jacket for baby [33]; (b) textile electrodes embedded into a baby suit [34]; (c) belt with embroidered electrodes [46]; (d) armband with embedded textile electrode [47]; (e) Bluetooth-enabled mobile ECG monitoring system integrated on a t-shirt [48]; (f) t-shirt embedded with textile electrodes and a local portable device [35]; (g) t-shirt with embroidered electrodes [49]	5
Figure 2.1 Action potential of a contractile cell[50].....	10
Figure 2.2 Conducting system of the heart [50]	11
Figure 2.3 The limb leads of heart signals.....	12
Figure 2.4 The chest leads[54].....	13
Figure 2.5 Electrical events of the cardiac cycle (P wave, QRS complex and T wave) [55].....	14
Figure 3.1 Electrode- electrolyte junction for pre-gelled Ag/AgCl electrodes.....	17
Figure 3.2 Schematic representation of the path of biopotential signals starting from the skin surface until acquisition and display at the circuit output [adapted from[73]].	23
Figure 3.3 Equivalent circuit of skin–electrode interface for (a) traditional wet electrodes and (b) textile electrodes [adapted from [74]].	24
Figure 3.4 Primary methods of realizing conductive textiles [14], [22], [23], [95], [96], [97].....	28
Figure 4.1 RGO synthesis steps from oxidation to reduction[149]	38
Figure 4.2 Schematic summary of graphene textile coating processes	40
Figure 4.3 Raman Spectrum Analysis for Graphene Electrode.....	41
Figure 4.4 SEM images of graphene coated textile electrodes.....	41
Figure 4.5 Processes of graphene armband preparation	42
Figure 4.6 Raman spectra results of graphene coated armband and graphene oxide(GO) coated armband.....	43

Figure 4.7 SEM images of graphene armband	44
Figure 4.8 The hardware level schematic of the analog section of the signal conditioning unit and block diagram of the developed ECG system for real-time monitoring and recording.....	46
Figure 4.9 Integrated system of graphene armband with ECG acquisition circuitry	48
Figure 4.10 Integrated system of graphene garment with ECG acquisition circuitry	49
Figure 4.11 Comparison skin electrode impedance values with Ag/AgCl electrode and graphene textile armband.....	50
Figure 4.12 Conductivity measurement results for different length and different part from graphene coated textile.....	50
Figure 5.1 Experimental setup showing the simultaneous acquisition of ECG from the subject with graphene textile armband and plot of the recorded signals for three cases are sitting, standing and walking for 300 seconds.....	53
Figure 5.2 Graphs of ECG recordings obtained using graphene textile and Ag/AgCl electrodes that displayed the highest correlation among the 3 cases on 8 different participants; the unique eye movement patterns acquired from participant 1 using graphene textile electrodes; and (c) Ag/AgCl electrode	54
Figure 5.3 Some of participants	55
Figure 5.4 (a) Comparison of Beat per minute (BPM) value between clinical device and graphene textile electrode and (b) Taken ECG signal wave (P wave-QRS complex-T wave)	56
Figure 5.5 Graphs of ECG signals taken from two participants in three different positions; sitting, standing and walking and correlation values between Ag/AgCl electrodes and graphene textile armband.....	58
Figure 5.6 Graphs of ECG signals from his arm (a) in the air, (b) in the 180 degree position, and (c) in the 90 degree position.....	59

LIST OF ABBREVIATIONS

ECG: Electrocardiogram.....	1
Ag/AgCl: Silver/Silver Chloride.....	1
Cu: Copper.....	3
Ni: Nickel.....	3
PVD: Physical Vapor Deposition.....	3
Ti-PET: Titanium–Polyethylene Terephthalate.....	3
PEDOT: PSS: Poly (3,4-Ethylenedioxythiophene) Polystyrene Sulfonat.....	3
RA: Right Arm.....	3
LA: Left Arm.....	3
LL: Left Leg.....	3
IoT: Internet of Things.....	3
mHealth: Mobile Health.....	4
BCI: Brain-Computer Interfaces.....	4
HMI: Human–Machine Interfaces.....	4
HCI: Human–Computer Interfaces.....	4
PC: Personal Computer.....	4
E_{hc} : Half Cell Potential.....	21
EMG: Electromyography.....	24
DSP: Digital Signal Processing.....	24
ICPs: Intrinsic Conductive Polymers.....	28
PANI: Polyaniline.....	28
PPy: Polypyrrole.....	28
ECPs: Extrinsicly Conductive Polymers.....	28
PU: Polyurethane.....	30
CNT: Carbon Nanotube.....	31

MWNT: Multi-Walled Carbon Nanotube.....	31
SWNT: Single-Walled Carbon Nanotube.....	31
R2R: Roll to Roll	32
GO: Graphene Oxide	36
rGO: Reduced Graphene Oxide	37
SEM: Scanning Electron Microscope.....	38
GUI: Graphical User Interface.....	43

1. INTRODUCTION AND MOTIVATION

1.1. Introduction

Due to the increase in cardiovascular health problems, efforts have been placed on developing wearable health monitors that continuously monitor heart activity and related bio-potential signals. By attaching conductive electrodes on suitable locations across the body, the surface bio-potentials occurring due to natural cardiac activity can be measured for a period forming the electrocardiogram (ECG) [1]. For ECG measurements, the most widely used bio-potential electrodes are the silver/silver chloride (Ag/ AgCl) “wet” electrodes which are supported by an adhesive backing and gel layer to improve contact with the skin. However, the use of “wet” electrodes in wearable long-term monitoring applications (e.g. Holter monitors) is often not preferable due to the skin irritation and discomfort caused by the gel; and the potential measurement errors due to decline of electrode performance and conductivity as the gel dries with time [1].

To address the requirements of long-term health monitoring applications, there has been growing interest to develop skin-compatible, wearable, “dry” bio-potential electrodes that eliminate skin irritation, discomfort and issues with gel-drying encountered in commercial electrodes [2]. Owing to their soft texture, comfortable feel, and ability to be directly weaved into clothing; textile materials and fabrics can be inherently advantageous to construct dry, gel-free, flexible, wearable devices including bio-potential electrodes and sensors for electrocardiogram monitoring [3]. However, alongside these advantages, there have been several challenges against successful realization of textile-based bio-potential electrodes for wearable applications.

The first challenge is on the technological difficulties of imparting conductivity to ordinary textiles in large sizes weaved from non-conductive fibers including nylon, cotton, and polyester; while still maintaining the soft texture of the original textile. To develop conductive textiles for bio potential monitoring applications different methods have been investigated which include metal deposition and electroplating [4],[5],[6], screen printing of conductive pastes on fabrics [7],[8],[9],[10], and knitting of fabrics with metallic fibers [11],[12],[13]. These approaches have rather limited scalability either due to equipment or process requirements and may trade-off the softness and texture of the textile while imparting electrical conductivity. In our earlier work, we have addressed this issue by merging graphene with conventional textiles using a low-cost, scalable approach and pioneered the development of conductive graphene textiles with stable electrical properties for ECG acquisition [14].

The second challenge is to ensure proper signal acquisition even under the presence of motion. ECG recordings can serve as a good indicator of heart activity and are useful for early diagnosis of cardiac diseases only if high fidelity signal acquisition is permitted by the electrode. However, ECG signals are usually distorted by different sources such as powerline or 50 Hz noise, high frequency noise and motion artifacts [15]. Most of the distortions can be filtered out using nominal frequency filtering techniques; but motion artifacts are difficult to be isolated from the ECG signal, since the artifact and the ECG signal have overlapping frequency spectra. On the other hand, the ECG signal extracted from textile electrode is more susceptible to motion artifacts in comparison to conventional electrodes. Fortunately, various techniques are being investigated to suppress motion artifacts and still permit accurate ECG acquisition even under motion [16].

The third challenge, which is often overlooked, is on the system-level integration of textile-based bio-potential electrodes with clothing and electronics, while maintaining maximum wearability. Considering the shape of the human body, only few locations primarily in the limbs, remain for successful recording of the electrocardiogram with a wearable, lightweight, portable, ergonomic device that can be attached to the body as a fashionable accessory. However, the magnitude of the cardiac vector has varying strength across the body which places additional design constraints on the electronics, signal processing and sensor locations.

1.2. Related Work

With the increase in cardiovascular diseases, there has been a growing interest in developing wearable devices that can continuously monitor cardiac activity. According to the World Health Organization, heart problems are the number one killer worldwide, accounting for 31% of total deaths each year (~17.9 million) [17]. Cardiovascular diseases assessed through abnormalities in heart rhythm such as atrial fibrillation, ventricular fibrillation, and atrioventricular block require long-term monitoring [18]. As people diagnosed with cardiovascular diseases have a higher rate of mortality in comparison with healthy people, the need for wearable devices that enable continuous heart monitoring is critical for a quick emergency response and earlier detection of heart malfunctioning [19].

Table 1.1 Summary of the various integrated textile system solutions categorized based on the acquired biopotentials to show the different manufacturing techniques and conductive materials used in their realization and the active sensing regions on the body

Biopotential Signal	Manufacturing Technique	Conductive Material	System Integration	Electrode Location	
[3]	ECG	Sputtering, electroless plating, knitting, and embroidering	Cu, Ni, stainless steel filament, nylon fabric	T-shirt	Chest
[14],[20]	ECG	Graphene-coated textile	Graphene	Wristband	Left and right arms
[21]	ECG	Electroless plating	Silver nanoparticles	Smart garment	Lead 1 and 2
[22]	ECG	Weaving and knitting	Silver yarns	Chest band	Chest
[23]	ECG	Knitting	Silver, stainless steel yarn, copper filaments	Garment band	Lead 1
[24]	ECG	Knitting, embroidering, and weaving	Silver	Elastic belt	Chest
[25]	ECG	Knitting	Stainless steel	Belt	Chest
[26]	ECG	PVD	Ag/Ti-PET yarn	Belt	Chest
[27]	ECG	Conductive thread	Silver, PEDOT: PSS	Bras	Lead 1 to 3
[28]	ECG	Printing	Silver	Chest band	Chest
[29]	ECG	Ink-jet printing	Graphene	T-shirt	Finger
[30]	ECG	Commercial textile	Silver	T-shirt	Lead 1 to 3
[31]	ECG	Screen printing	Silver paste	Band-Aid	Chest
[32]	ECG	Knitting	Silver coated yarns	Swimsuit	Chest
[33]	ECG	Commercial textile	Silver and gold	Smart jacket	Chest
[34]	ECG	Knitting and woven	Stainless steel	Baby suit	Back
[35]	ECG	Knitting	Stainless steel threads	T-shirt	RA, LA, LL, RL, V1-V6

Among the various applications of e-textiles, cardiac biopotential monitoring is growing steadily and shows large parallelism to the developments in wearable technologies and the internet of things (IoT) [36],[37]. Applications from mobile health monitoring (mHealth) to brain–computer interfaces (BCI) and human–machine/computer interaction (HMI/HCI) are greatly facilitated by developments in wearable technologies, and in this respect, textile electronics is a key technology enabler. Since a critical signal “source” in wearable applications is the human body itself, in this section, we focus on providing an overview of the cardiac biopotentials that have been acquired by conductive textiles and discuss the relevant applications (Table 1).

ECG is a biopotential signal acquisition method by which the variation in heart potential is measured by utilizing surface electrodes across the body. It is a non-invasive method and gives a thorough indication of any abnormalities in heart rhythm. Its main components (i.e., P-QRS-T complex) can be used to diagnose various cardiac disorders. For instance, missing P-waves is an indication of atrial fibrillation and can lead to stroke; arterial diseases can be revealed by the morphology of the ST segment duration; variation in RR intervals leads to sleep apnea; abnormality of QT intervals is attributed to ventricular fibrillation and causes sudden cardiac arrest [38]. While some of these abnormalities are not immediately fatal and can be detected over longer diagnostic periods, others are characterized by sudden changes in ECG signal (e.g., ventricular fibrillation) and cannot be detected unless continuous monitoring is practice [18]. A wearable routine monitoring system can help resolve this issue without restricting patients to a static ECG monitor.

From the perspective of wearability, textile substrates offer integration between various system modules such as electrodes, microprocessors, and transceivers. Therefore, they are helpful for offering a robust solution to realize smart clothing for personalized, point of care health monitoring. Textile platforms for wearable and continuous monitoring of ECG have been extensively studied [20],[30],[31],[39],[40]. Some of these wearable clothes are waterproof [32], while others were developed to encourage exercising and fitness through the routine monitoring of daily activities [41]–[43]. Among these projects, MagIC Space was a promising work designed to monitor heart activity and other vital signs while sleeping on space stations [44].

Moreover, conventional electrodes in a neonatal intensive care unit cause possible irritation and discomfort for neonates and requires separating them from their mother since they always need to be connected to the monitoring system .

It has been shown that a wearable monitoring system with textile electrodes designed for babies can increase the comfort of both the baby and the mother (Figure 1.1a,b) [33], [34], [45]. Moreover, textile electrodes are implemented in different forms such as belts (Figure c) [46], armbands (Figure 1d) [47], and t-shirts (Figure 1.1e–g) [35], [48], [49].



Figure 1.1 Wearable electrocardiography (ECG) systems: (a) jacket for baby [33]; (b) textile electrodes embedded into a baby suit [34]; (c) belt with embroidered electrodes [46]; (d) armband with embedded textile electrode [47]; (e) Bluetooth-enabled mobile ECG monitoring system integrated on a t-shirt [48]; (f) t-shirt embedded with textile electrodes and a local portable device [35]; (g) t-shirt with embroidered electrodes [49]

1.3. Summary of Work

For wearable monitoring systems to be more usable and widespread, the user must be able to use and wear the system easily, comfortably and without preparation. The designed system does not require preparation in advance, but it must be correctly

positioned to ensure good electrical contact with the skin. Thus, motion artifact problems can be minimized. Our wearable system does not cause any discomfort or skin irritation but can be reused and machine washed. In a wearable biopotential monitoring system it is not easy to provide all these features. In addition to the well-designed electronic system, the electrode design needs to be admirable.

In order to measure the ECG signal and heartbeat in different situations, we developed a wearable system prototype using conductive textile formed by coating graphene with different techniques on textile. Ag / AgCl electrodes, which are used as standard, are both allergic and irritating to the skin due to their gel structure and are not suitable for long term signal reception due to gel drying. It is also a disadvantage that it is disposable. For this purpose, the performance of the conductive textile armbands, skin impedance compared to conventional Ag / AgCl electrodes. In signals received from subjects in many different situations, it has been found that conductive arm bands perform similar to conventional electrodes. To increase wearability, the conductive armband is taken from the top of the left arm. The signal information received from the wearable conductive armband can be easily transferred to the PC (Personal Computer) via Bluetooth and can be monitored via an interface.

1.4. Outline

In this section, general information about the thesis and studies are given. Chapter 2 provides background information on the electrical activity of the heart and heart signal reception, ECG measurement system, and leads.

In Chapter 3, electrodes and working mechanisms used in ECG measurements and their studies are mentioned. In addition, how textile electrodes are produced, the reasons affecting these electrodes and production techniques are discussed in detail.

Chapter 4 describes the preparation of graphene-coated textile electrodes and a direct patterned conductive garment using the stencil printing technique on the armband, and details of the signal acquisition system for ECG signal acquisition and how to combine

them into a prototype. In addition, the study on the comparison of the skin electrode impedance of the Ag / AgCl conventional electrode and graphene coated electrodes is presented.

In Chapter 5, the comparison of ECG signals from different people and the correlation values with Ag / AgCl electrodes are presented.

2. BACKGROUND ON ELECTROCARDIOGRAM

2.1. Electrical Activity of Heart

The heart is a myocardium covered with thin outer and inner layers of the heart muscle or epithelium and connective tissue. Heart muscle cells are connected at two types of intersections. The right and left sides of the heart are separated by the interventricular septum, so that the blood on one side does not mix with the blood on the other side. The dissociations hold the cells together, and the gap junctions allow the action potential to propagate from one cell to the adjoining area. The heart muscle cells are stimulated by autorhythmic cells of the heart and are therefore activated without any conscious movement. The distinctive feature of myocardial action potential from the action potentials in other muscle cells and nerve axons is the long plateau stage [50].

Electrical activity in the heart is produced in SA node, AV node and Purkinje cells. The SA node is the stimulus center of the heart and consists of functional myocardial cells. In these non-resting cells, depolarization, called the pacemaker potential occurs slowly and spontaneously during the diastole period.

The action potential begins as a result of the activity of the ion channels in the heart cell membrane. Spontaneous depolarization arises due to ion channels opened in response to hyperpolarization. These channels are permeable to both Na^+ and K^+ ions. Both Na^+ and K^+ ions can pass through this channel. The influx of Na^+ ion into the cell creates depolarization. When the membrane potential reaches the threshold, it causes the voltage-gated Ca^{2+} channels in the plasma membrane of the pacemaker cells to open, and gradually reaches the voltage capacity of a Ca^{2+} channel opened with membrane potential around -50 mV. By the opening of the channels, the Ca^{2+} ion enters the pacemaker cells,

that causes contraction in myocardial cells [50].

It is resulted in repolarization when K^+ ion exits the cell through voltage-charged K^+ channels. A myocardial cell produces its own action potential after being stimulated by its potential from the SA node. When the depolarized myocardial cell reaches the threshold degree, the voltage-loaded Na^{2+} channels are opened by the action potential from the SA node. The membrane potential is returned to -60 mV to initiate the next action potential. system of specialized myocardial cells is responsible for transporting the action potentials exiting the SA node. The transmission system of specialized myocardial cells is responsible for transporting the action potentials moving the SA node. This transmission system consists of an AV node, his bundle and Purkinje fibers. The generated action potential is quickly transmitted through the internodal paths to the AV node located at the base of the right atrium. The AV node is responsible for the connection between atrial depolarization and ventricular depolarization. The action potential passes through the AV node for short delay. This delay ensures complete contraction of the atria before the ventricles begin to stimulate. Once the AV node has become stimulated, the action potential is propagated downwards through the interventricular septum through the conduction fibers called His bundle. The bundle of His is divided into the right and left bundle branches which are separated from each other in the apex of the heart in the interventricular septum and which enter the walls of both ventricles. These bundle branches also branch out as Purkinje fibers, which are widely distributed within the ventricles. Purkinje fibers rapidly distribute the stimulus in the ventricular myocardial cells. It spreads its potential to the ventricular myocardium from the inside to the outside, allowing simultaneous contraction of the two ventricles and simultaneously pumping blood into the pulmonary and systemic circulation[51].

The action potentials leaving the SA node are propagated using internodal paths by the atrium at a rate of about 0.8 to 1 m / sec. When it comes to AV node, its speed decreases to 0.03-0.05 m/s. The stimuli passing through the AV node accelerate in the His bundle and reach up to 5 m/s in Purkinje fibers. Ventricular systole starts 0.1-0.2 sec after atrial systole with such rapid delivery of stimuli [52].

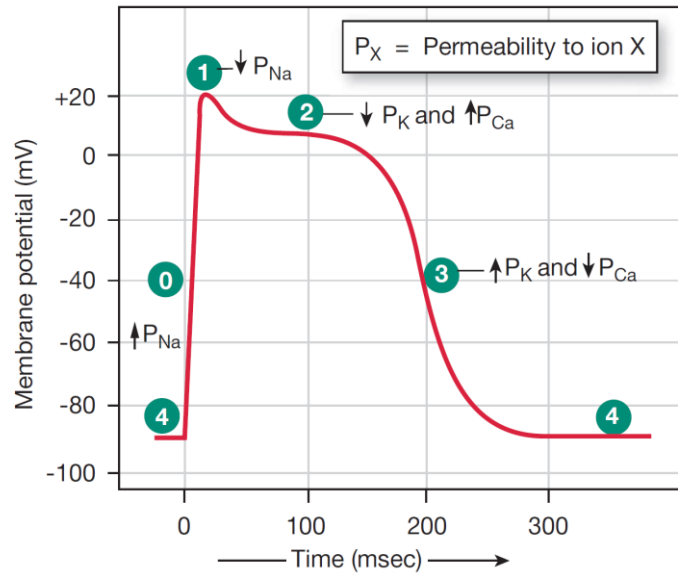


Figure 2.1 Action potential of a contractile cell[50]

As shown in Figure 2.1, the Na^+ input leads to the rapid depolarization phase of the action potential, while the K^+ exiting the cell leads to the vertical repolarization phase. Four phases are explained as detailed below. Phase 4 is the resting membrane potential phase. The resting potential of myocardial contraction cells is approximately -90 mV. Phase 0 is the depolarization phase. When a depolarization wave enters a contractile cell through hollow junctions, the membrane potential becomes more positive. Voltage-gated Na^+ channels need to be opened for Na^+ to enter the cell and thus depolarizing event occurs rapidly. The membrane potential reaches +20 mV before the Na^+ channels are closed. Phase 1 is the initial repolarization. When the Na^+ channels are closed, the cell begins to repolarize as K^+ passes through the open K^+ channels. Phase 2 is the plateau phase. Initial repolarization is very short. The action potential is then flattened on a plateau as a result of two events. A decrease in K^+ permeability occurs, and an increase in Ca permeability is observed. The voltage-gated Ca^{2+} channels activated by depolarization slowly open in phases 0 and 1, causing Ca to enter the cell. At the same time, some fast K^+ channels are turned off. As Ca^{2+} flow increases, K^+ decreases and the movement potential become flat on a plateau [50]. Phase 3 is the rapid repolarization phase. The plateau ends with the closure of Ca^{2+} channels and increased K^+ permeability. When the slow K^+ channels are turned on, K^+ quickly exits and returns the cell to resting potential, and the system returns to baseline (phase 4).

Anatomy of the heart and circulation of the conduction system are shown in figure 1.2. As shown in figure 2.2, firstly (1) the electrical potential that begins at the SA node is depolarized. Later (2), the electrical potential then travels rapidly through the internodal paths to the AV node, and depolarization spreads more slowly in the atrium. In the 3rd case, the transmission slows along with the AV node. Next (4), depolarization rapidly moves from the ventricular conducting system to the top of the heart. Moreover, finally (5) the depolarization wave propagates upward from the peak [50].

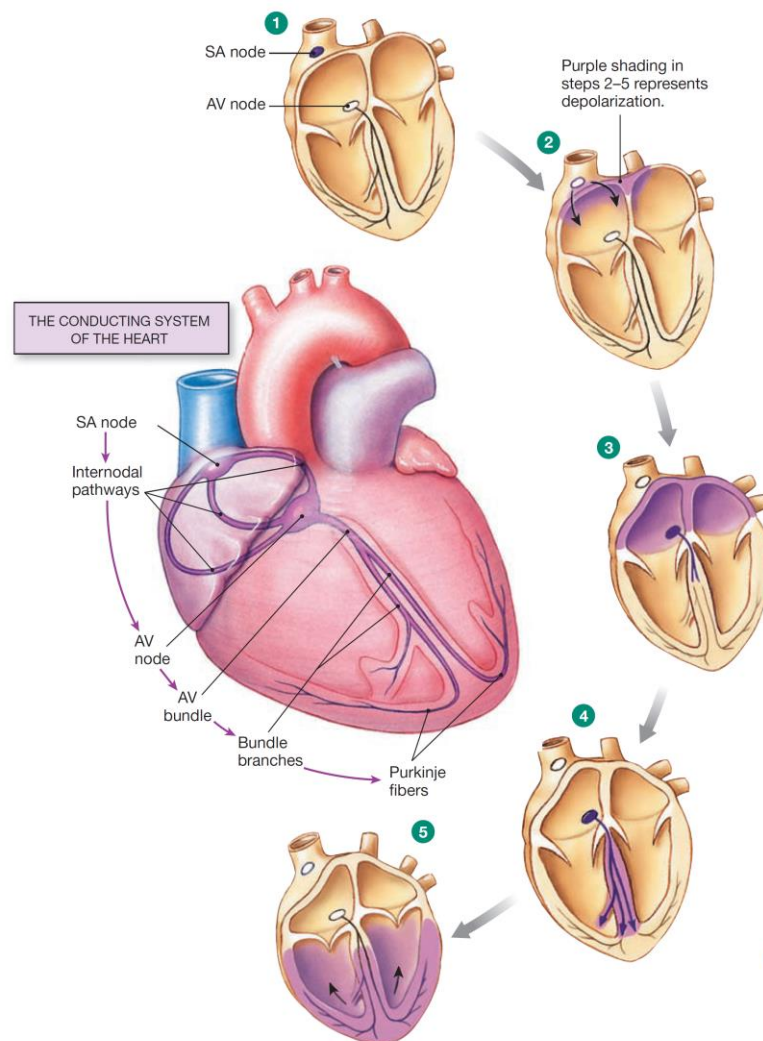


Figure 2.2 Conducting system of the heart [50]

2.2. ECG Signal Measurement and Lead Points

The first human electrocardiogram was recorded in 1887. Later, in 1903, Willem Einthoven (1860-1927) found the galvanometer and succeeded in printing the heart signals. He created the triangle of Einthoven by placing both the arm and the left leg of the electrodes around the heart, as shown in Figure 2.3. According to the Einthoven theorem, three limb electrodes are connected to a voltmeter [53]. The edges of the triangle are numbered to correspond to the three wires or electrode pairs used for recording. One electrode represents the positive part in one lead, while the other electrode represents the negative part.

When a moving heart wave travels towards the positive electrode, the ECG wave goes up, but when it is the opposite, i.e. when the electric wave travels towards the negative electrode, the ECG wave goes down. The action potential and the ECG signal do not have the same amplitudes. ECG consists of waves and segments. While waves occur below or above the baseline, segments arise from between two waves of the baseline. Intervals originate in of a combination of waves and parts.

Different ECG waves refer to depolarization and repolarization of the atrial and ventricle. In a conventional ECG signal, the electrical activity of the heart is monitored from 12 leads: six limb leads and six chest leads [52]. According to Einthoven's theorem, an ECG signal can be recorded in three different combinations called three bipolar limb leads, designated lead I, lead II and lead III [50]. In the Lead I, the negative electrode is connected to the right arm while the positive electrode to the left arm.

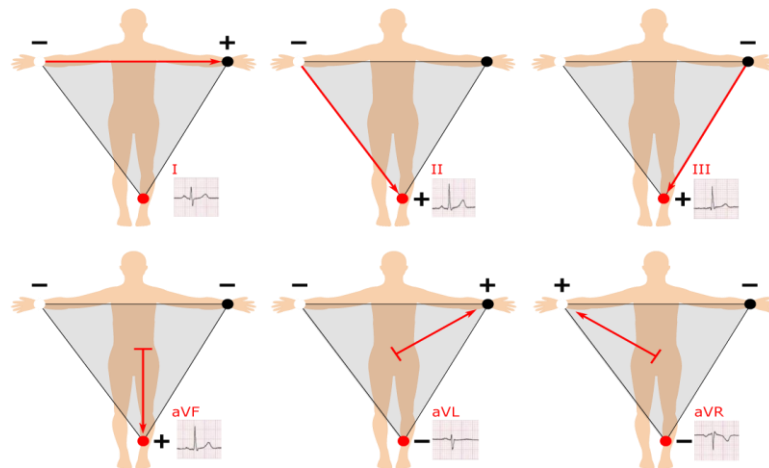


Figure 2.3 The limb leads of heart signals [54]

The first wave in an ECG recorded in Lead I is the P wave corresponding to depolarization of the atria. The progressive ventricular depolarization wave assigns the QRS complex. Finally, the T wave describes the repolarization of the ventricles. Atrial repolarization does not represent a distinct wave but is included in the QRS complex. Waves may vary in different leads. In II, the negative electrode of the ECG is connected to the right arm while a positive electrode is placed on the left leg. Finally, III. in the lead, the negative electrode is placed on the left arm, and the positive electrode is placed on the left leg. As a result, when the negative side is measured negative to the positive side, the ECG will be recorded as positive.

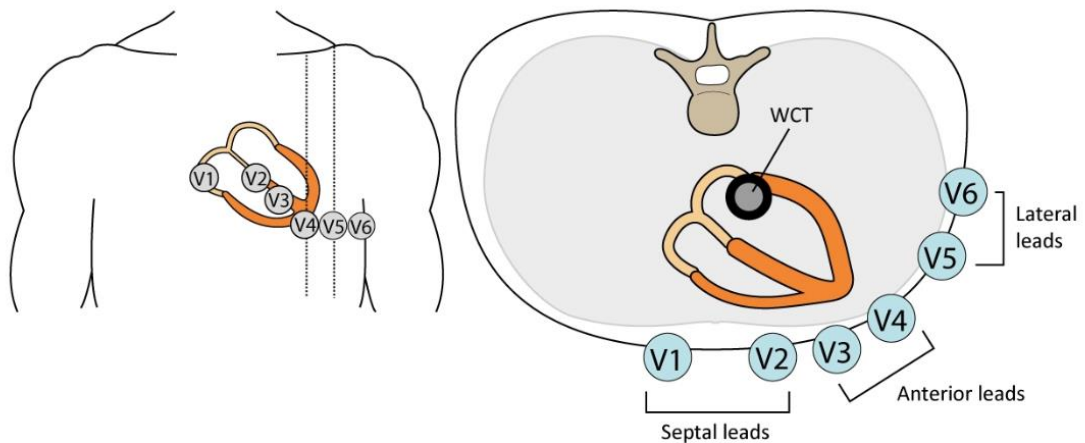


Figure 2.4 The chest leads [54]

In addition, ECG signal reception is performed using chest electrodes. For this, there are six chest points V_1 , V_2 , V_3 , V_4 , V_5 and V_6 as shown in figure 2.4. The unipolar aVR , aVL and aVF , are also referred to as augmented limb leads. Since the results are very small, the signals are increased. Goldberger's aVL , aVR and aVF are mathematically related to Einthoven leads. The equations are;

$$aVL = \frac{\text{Lead I} - \text{Lead III}}{2} \quad (1.1)$$

$$-aVR = \frac{\text{Lead I} + \text{Lead III}}{2} \quad (1.2)$$

$$aVF = \frac{\text{Lead II} + \text{Lead III}}{2} \quad (1.3)$$

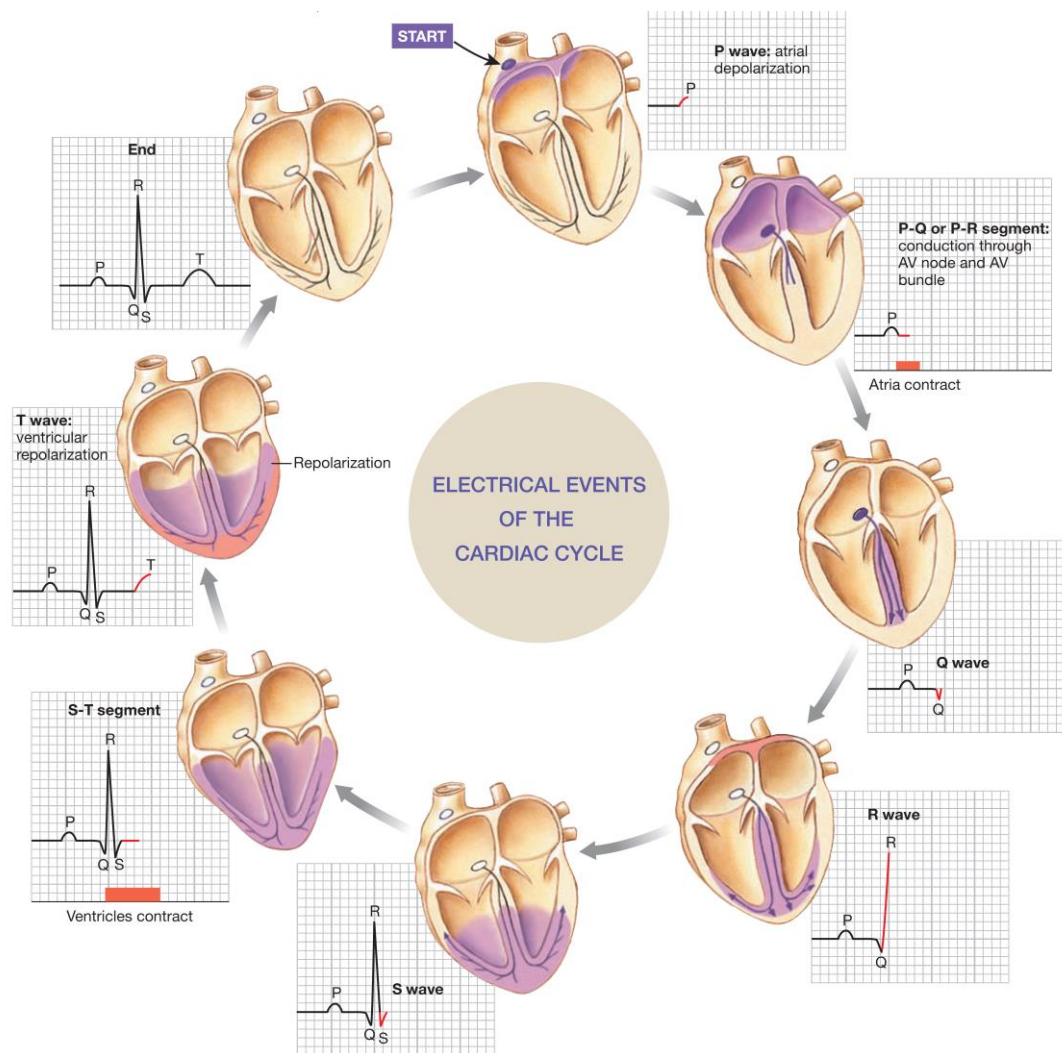


Figure 2.5 Electrical events of the cardiac cycle (P wave, QRS complex and T wave) [55].

The heart cycle begins at rest with both the atrium and ventricles. The ECG signal begins with atrial depolarization. Atrial contraction begins in the second part of the P wave and continues in the P-R segment. During the P-R segment, the electrical signal slows as it passes through the AV node and the AV beam. Ventricular contraction begins immediately after the Q wave and continues along the T wave. The ventricles repolarize during the T wave, followed by ventricular relaxation. During the T-P segment, the heart is electrically silent. A series of intervals from an ECG record can be measured and analyzed with a normal signal that provides crucial information about expelled into

arteries, which normally last for about 0.35 seconds. During the Q-T interval, which represents the time between the Q point and the starting point of a T wave, the ventricles are in a depolarized state. It is the R-R (beat-to-beat) interval that specifies the time between two consecutive QRS complexes, the interval indicating the heart rate. Finally, the S-T segment, which lasts from the S-point to the onset of the T-wave, is a very important range for diagnosing heart-related problems such as heart attack or depression in individuals with coronary problems. Detail electrical events of cardiac cycle is shown in figure 2.5. In general, ECG recording provides basic information for the assessment of cardiac anomalies [56].

3. ELECTRODES FOR ELECTROCARDIOGRAM

3.1. Conventional Electrodes

Augustus D. Waller made his first ECG measurement by placing his hands and feet in buckets filled with saltwater to act as electrodes. There is an interface between signal source and the monitoring system that collects signals from the body. This interface, called the electrode, is in direct contact with the body. This electrode converts the ionic current in the body into an electron current. Ag / AgCl electrodes with non-polarizable electrodes and adhesive gels are used in clinics because of their stable properties. Conventional Ag / AgCl electrodes consist of three main areas: electrolyte gel, adhesive pad and the metallic layer. The conductive part of the electrode is usually a silver wire coated with a thin layer of silver chloride. In the ECG measuring device, two or more electrodes are placed on the skin, acting as an electrolyte.

The half cells are then connected together by an electrolyte to form an electrochemical cell. A voltmeter measures the net potential. A separate conductive gel is also applied between the tip of the silver plate on the electrode and the skin to provide a path for current flow [57].

An interaction between the electrode and the electrolyte is necessary for the electrical current to continue through the interface. Thus, the ionic current can be converted into the electron current. In order to characterize the interface between the electrode and the electrolyte in the electrochemical redox reaction system, it contains an electrolyte solution containing cations and anions and an electron electrode [3].

The oxidation reaction occurs when the metal oxidizes and dissolves the electrolyte to give an electron to the electrode. As shown in equation 3.1 and 3.2, the anion is oxidized to a neutral atom by giving electrodes from the electrode. The reduction reaction occurs when the cation C^+ receives an electron to C and the Anion A to A^- as shown in figure 3.1 [56].

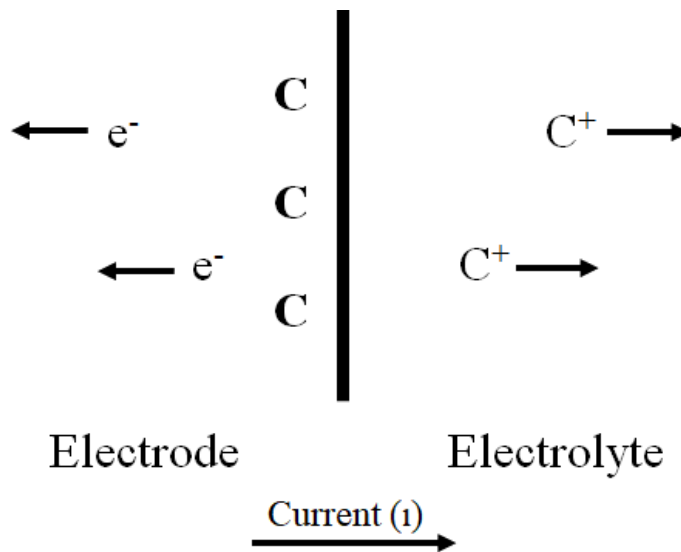


Figure 3.1 Electrode- electrolyte junction for pre-gelled Ag/AgCl electrodes (modified from [56]).



where n is the valence of C , m is the valence of A [56].

Through the exchange of electrons during the redox reaction, the current continues through the interface. Oxidation is more effective when the current flows from an electrode to the electrolyte, but the reduction is effective for the opposite case, ie when current flows from the electrolyte to the electrode.

According to above equations, reactions of Ag/AgCl electrodes equations can be written as;



The half-cell potential of the Ag / AgCl electrode is explained by the Nernst equation[56]. Equations are followed by;

$$E = E_{Ag}^0 + \frac{RT}{nF} \ln a_{Ag^+} \quad (3.5)$$

$$E = E_{Ag}^0 + \frac{RT}{nF} \ln \frac{K_s}{a_{Cl^-}} \quad (3.6)$$

where E is the standard reduction potential, R is gas constant, T is absolute temperature, N is number of involved electrons, A is activity of involved compounds, and F is faraday constant.

Conventionally, biopotential signals are measured by disposable, “wet” silver/silver chloride (Ag/AgCl) electrodes [58]. Wet electrodes are comprised of a gel layer to reduce the skin–electrode contact impedance and adhesive padding to improve contact with the skin. The performance of wet electrodes, however, degrades with time as the gel layer dries, which further results in degradation of the signal fidelity. In addition, wet electrodes usually require skin preparation, which can involve the abrasion of the outer skin layer [59]. On the other hand, the gel can cause allergic reactions and irritation, while the adhesive layer causes added discomfort both while wearing the electrode and at the time of removal, due to the need for mechanical peeling for electrode detachment [2],[60].

3.2. Dry Electrodes

Dry electrodes do not contain any electrolyte layer except skin sweats. The dry electrodes are divided into two as contact or non-contact, and the interfaces of these electrodes are somewhat difficult and complex to explain. Dry electrodes can provide a galvanic or capacitive electrical current path when in direct contact with the skin [55].

Various studies have been reported in the literature from dry stainless-steel discs to electrodes produced using MEMS technology [2]. Due to the small-signal amplitude of the ECG, the performance of the electrodes produced for recording the ECG signal is of great importance. Both conductivity and capacitance play a critical role in characterizing electrode performance. Metal has been the most widely used material in dry electrode studies. Flexible versions of the dry electrode based on rubber [61],[62], fabrics [14] or foam [63],[64] are also possible and are more attractive than dry metal electrodes for both comfort and useable. Because the metal can irritate the skin in long usage. Soft materials have the advantage of easily adapting to the skin, increasing comfort and contact area.

3.2.1. Contact Electrodes

The electrode should remain as stable as possible in order to avoid movement artifact in the signal when the user receives the ECG signal. The electrolyte in the contact electrode is moisture in the skin. In order to solve the problem of motion artifact in the dry electrodes, a foam electrode having high stability and excellent stability was produced [65]. The stratum corneum, the high-resistance layer of skin, can be abraded or hydrated to provide lower resistance and better electrode contact. With the advances in MEMS technology, it has become possible to penetrate the very thick layer with microfabric needles [66], [67]. However, these needles are not very useful as they can cause some problems in the skin when it stops for a long time[65].

In order to make the electrodes more flexible and wearable, polymers have been used as the substrate in electrode production, and studies have been conducted to combine conductive polymer electrodes with metal particles [68], [69].

3.2.2. Non-contact Electrodes

Non-directly coupled dry electrodes are contemplated to be capacitively coupled. A non-contact dry electrode is specified as conductive material deposited by an electrically insulating layer. These electrodes can behave as a capacitively coupled electrode when touched directly on the skin surface. Non-directly coupled dry electrodes are dealt with to be capacitively coupled. Capacitively connected electrodes can detect biological potentials in that region. These electrodes only operate with displacement currents and therefore, cannot transmit reduced frequency signals [55].

The non-contact electrode can detect signals in the space between the sensor and the skin. Thus, without the need for a particular dielectric layer, the ECG signal can be received through insulation such as hair or air. Furthermore, these electrodes are generally defined as coupling signals over small capacitance [2]

Furthermore, in these electrodes, the electrical current in the conductive electrode through the capacitive coupling between the electrode and the skin separated by a dielectric layer is provided by the displacement current flowing through the skin. However, non-contact electrodes exhibit poor deposition times due to the high permeability of the electrode. Furthermore, in these electrodes, the electrical current in the conductive electrode through the capacitive coupling between the electrode and the skin separated by a dielectric layer is provided by the displacement current flowing through the skin [70], [71]. However, non-contact electrodes performance impoverished deposition times because of the high permeability of the electrode. In some of the studies, stainless steel, aluminium or

titanium was used to structure a considerable blockade capacitor in series with the skin [72]. The signals are capacitively connected to the input of a FET (field effect transistor) buffer amplifier and then connected to standard devices. In another study, it produced an insulated electrode integrating a buffer amplifier [73].

3.3. Textile Electrodes

Although wet electrodes are standard in clinical environments, gel-free, “dry” electrodes can serve as good candidates for wearable, long-term, point-of-care personal health monitoring applications and many other similar systems. To this end, wearable conductive textiles provide a viable alternative. Therefore, it is the aim of this study to survey and critically review the state-of-art wearable textile technologies, with a specific focus on the acquisition of biopotentials including cardiac, neural, muscular, and ocular signals, and to discuss some of the emerging applications enabled by their detection and processing.

3.3.1. Performance Characteristics

Understanding the major performance characteristics for wearable biopotential monitoring system is important to assess their utility in recording and for the development of electrodes with better performance. Some key performance metrics include skin–electrode contact impedance, noise immunity or susceptibility to motion artifacts, stability, and lifetime of the electrodes. Even though the system’s “wearability”, user comfort, and seamless integration are not numerical metrics, they are some of the most important points to be considered in system-level development.

3.3.1.1. Skin Electrode Contact Impedance

In biopotential recordings, skin–electrode contact impedance is critical as it directly affects the received signal at the amplifier output. The effect is analogous to the filtering of the actual biopotentials emanating from the body [74].

If we assume the skin–electrode contact impedance of both electrodes to be equal ($Z_1(w) = Z_2(w)$) and name it as $Z(w)$, and similarly, the amplifier input impedance is seen by each electrode to be the same ($R_{i1} = R_{i2}$), then the transfer function of the system $H(s)$ can be expressed as the ratio of the amplifier output (V_o) to the biosignals V_1 and V_2 emanating from the body, as shown in Figure 3.2.

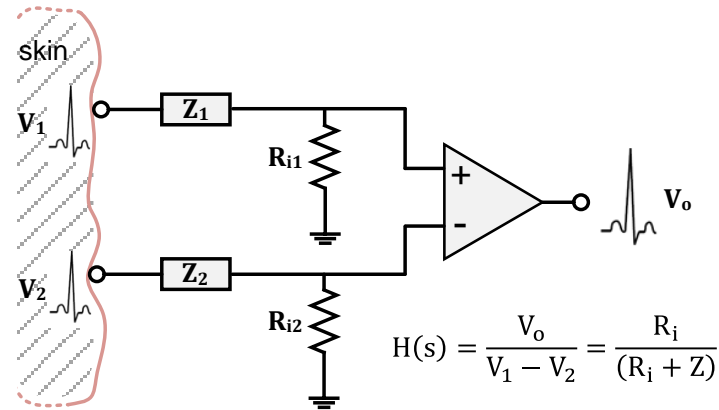


Figure 3.2 Schematic representation of the path of biopotential signals starting from the skin surface until acquisition and display at the circuit output [adapted from[74]].

An electrode–electrolyte interface can be modeled by a parallel RC network [56]. However, skin is more complex; understanding skin–electrode impedance and its frequency-dependent characteristics requires investigation of the skin itself, which consists of three main layers: epidermis, dermis, and hypodermis or subcutaneous tissue.

The outermost layer, the epidermis, plays a significant role in the skin–electrode interface since it has direct contact with the electrode, besides the fact that it constantly renews itself. The deeper layers involve the vascular tissues and the nerves along with sweat glands, sweat ducts, and hair follicles[75].

The equivalent circuit of the skin–electrode interface (Figure 3.3a) starts with an electrode half-cell potential E_{hc} followed by the electrode–electrolyte interface between the electrode and the gel, which is represented by capacitance due to electrical double layer formation C_d and charge transfer resistance R_d . The gel medium is modeled by a series resistance R_s . The upper layer of the epidermis behaves as a semipermeable membrane that causes the difference in ion concentration and a potential difference, which is shown

with E_{hc} . C_e and R_e model the impedance of the epidermal layer and R_a models the dermis, which behaves as a pure resistance.

Moreover, E_p , C_p , and R_p stand for the effect of sweat glands as a parallel conduction path through the epidermis [76]. The half-cell potential appears as a DC baseline on the biopotential signals and is a particularly important factor in design decisions for any physiological signal acquisition unit development. This is due to its fluctuation, as it varies even with a relatively insignificant movement in between the electrode and the skin, which is interpreted as a noise-like artifact.

Textile electrodes were believed to show a strong capacitive behavior compared to conventional electrodes, owing to the absence of electrolytes. Figure 3.3b illustrates this effect with capacitance C_t parallel to R_s , herein which C_t is in inverse proportion with sweat and the moisture over the skin [75]. Additionally, ambient humidity or applied pressure can be used to change moisture intensity [77]. Parallel RC blocks on the equivalent circuit imply that skin–electrode impedance decreases with increased frequency. The relation between acquired output signal and in-body biosignals means that lower frequency components of the biosignals will deviate more than the original. Decreasing the skin–electrode impedance, therefore, improves the signal quality.

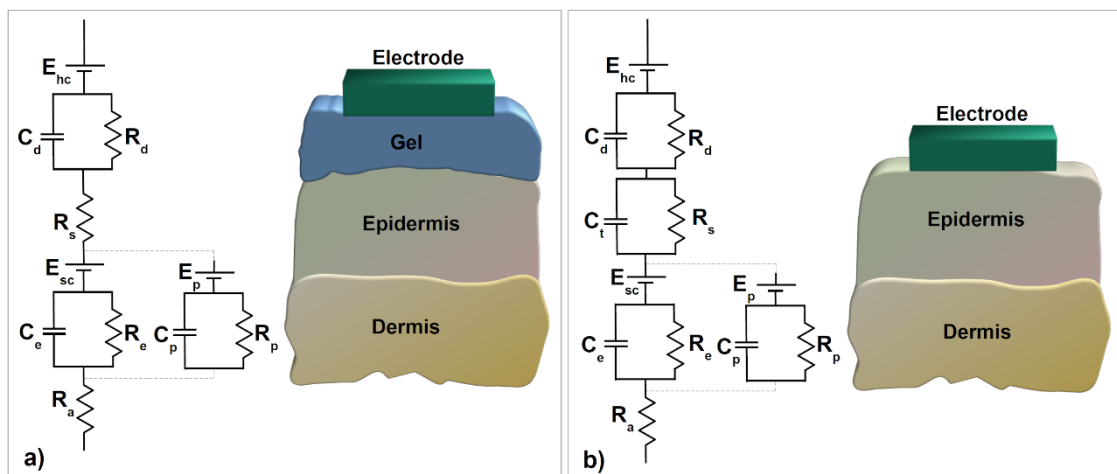


Figure 3.3 Equivalent circuit of skin–electrode interface for (a) traditional wet electrodes and (b) textile electrodes [adapted from [75]].

One way to decrease the skin–electrode impedance is by moisturizing the interface either with a hydrogel membrane or salty water. Since a membrane interface improves the comfortability of the electrode, instead of salty water, a hydrogel membrane seems more preferable. The only drawback of such a technique, however, is the bactericide/fungicide effect, which causes skin irritation, but by optimizing a hydrogel membrane’s pH value to between 3.5 and 9, this issue could be avoided [78]. The other ingredient that affects the skin–electrode interface is the electrode’s overall size, which presents an inverse relation with skin–electrode impedance [28]. In this manner, different sewing patterns affect skin–electrode impedance since they result in diverse contact areas. A comparison of knitted and woven textile electrodes showed that knitted textiles express lower impedance. Since sewing patterns directly affect density, their thread diameter ought to change the skin–electrode interface impedance [28]. Research has illustrated this fact, finding that in knitted structures, electrodes produced with a plain stitch had less impedance than electrodes produced with a honeycomb stitch since pits existing in honeycomb patterns represent non-contact areas[79]. In addition, studies have suggested that the pressure applied to the skin leads to lower skin–electrode impedance by providing better skin–electrode coupling [80].

It is, however, not an easy task to accurately compare skin–electrode impedance for different electrodes since people’s skin characteristics vary and can change with time [56]. Repeatable measurement setups are therefore desirable. It was suggested that the skin’s electrolytes can be simulated with an electrolyte cell, and electrochemical impedance spectroscopy can be used in electrode characterization [81]. A more comprehensive setup was suggested that uses a skin dummy made out of agar-agar [75]. It enabled contact impedance analysis at different frequencies and at different pressure levels.

3.3.1.2. Susceptibility to Motion Artifacts

Motion artifacts, identified as an undesirable signal in biopotential monitoring systems, occurs by any sort of motion due to movement of one part of a section with respect to another (e.g., movement of connecting cables, a patient’s head) and can be categorized in relation to five different sources[80].

1. Measurement of an unrelated biopotential signal, for instance, electromyography (EMG) interferences in an electrocardiography (ECG) recording. Proper electrode placement can usually avoid such interference [82].
2. Stretching of the skin leading to variations in the skin potential. In the textile electrode-based system, fixation of the electrodes relies on the applied pressure, which is in direct translation to the skin stretch. To reduce such motion artifacts, the applied force could be distributed to a bigger area than the electrode through the use of a supporting structure surrounding the electrode [83].
3. Motion between the electrical double layer of metal and electrolyte, which causes a voltage difference in its electrochemical cell. Reducing the electrolyte resistance, polarization potential, and the movement of the electrode are believed to decrease such motion artifacts.
4. Cable bending generating friction and deformation on the cable isolator, resulting in triboelectric noise [84]. To reduce this effect, a wearable garment or clothing could be designed in such a way as to secure cables and the acquisition system into the garment and provide wireless streaming of information.
5. Static electricity storage and discharge caused by patient or nurse-staff localization and/or movement [85].

Besides all of this, placing preamplifiers subsequently after the electrodes (i.e., active electrodes) is a recommended technique for reducing motion artifacts. A preamplifier block functions as an impedance converter that converts the high-impedance signal to a low-impedance one, lowering noise susceptibility and impedance mismatch before differential amplifiers [86]. Additionally, it is possible to use digital signal processing (DSP) algorithms for motion artifact reduction, including blind source separation and adaptive filters [80],[81]. Similarly, a multiscale mathematical morphology and finite impulse response bandpass filters were also shown to reduce the effects of motion artifacts [79].

3.3.1.3. Stability and Lifetime

The other expected requirement from textile electrodes is their stability and reusability, which directly affect their lifetime. In the literature, a few studies have looked into this

issue and characterize stability by subjecting their textile electrodes to “wash tests” with detergent, either by using a washing machine with respect to the ISO 6330 standard [87] or simply them dipping into detergent.

One of the factors that the washability of textile electrodes depends on is the adhesion of conductive material is on textile fibers. This issue will not occur for bulk conductive fibers like metal wires; however, they eventually create unwanted wrinkles and loops after cleaning in a washing machine [88]. Washing temperature, speed, and time are thought to have an effect on the adhesion of the conductive material. Therefore, an optimal washing range needed to be determined for the reusability of a textile electrode. Different groups have reported washing tests on textile electrodes, such as ones coated with Cu/Ni plating [89], PEDOT:PSS [90], graphene[14], and silver-based ink [91], which were reported to maintain their optimum stability even after multiple washing cycles.

3.3.2. Materials and Methods

While the materials and methods to realize conductive textiles do not directly affect the performance of the textile electrode, they are among the most important, if not the primary, aspects of e-textile technology since manufacturing cost and reliability tend to be a direct function of the manufacturing technology. In this section, a comprehensive survey of the various techniques and materials used to realize electroconductive textiles is provided. Fabrication of e-textiles essentially relies on the stable integration of conductive materials with fabrics and fibers. Commonly used conductive materials include metals, conductive polymers, and carbon allotropes (i.e., graphene and carbon nanotubes). These materials can be used either with mainstream fabric manufacturing/decoration approaches (e.g., knitting, weaving, embroidery) [13], or can be applied onto finished textiles with various techniques like electroplating [21], [92], physical vapor deposition (PVD)[4], [93], chemical polymerization [94], dip-coating [14], and printing methods [95] to coat the surface of the textile (Figure 3.4).

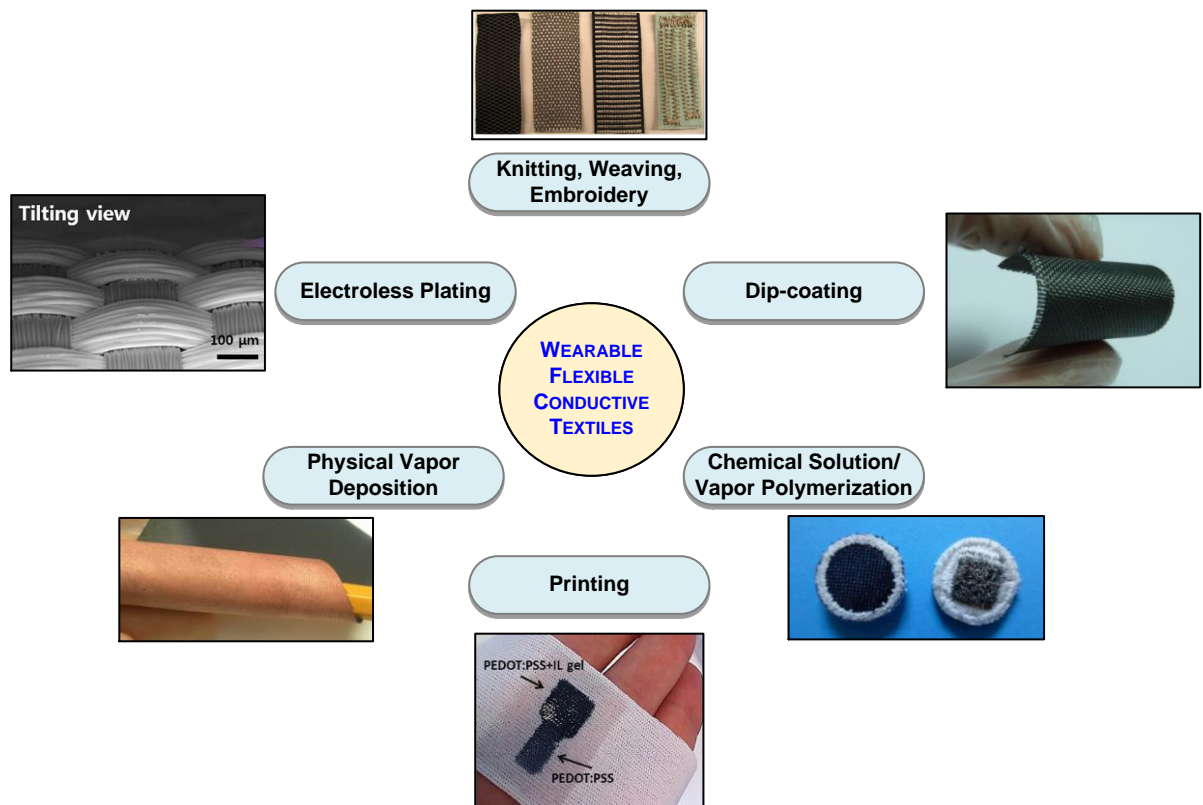


Figure 3.4 Primary methods of realizing conductive textiles [14], [22], [23], [95], [96], [97].

3.3.2.1. Knitting, Weaving, and Embroidery

Knitting, weaving, and embroidery are well-established techniques in textile manufacturing and decoration. By using various conductive fibers and yarns, e-textiles can be directly produced through knitting or weaving, while embroidery could be used to create conductive patterns on finished textile surfaces. Woven textiles are produced by interlacing two perpendicular sets of yarns. In contrast, knitting uses a needle to continuously connect a series of chains of yarn together. Embroidery is a decoration method for a finished fabric surface involving different forms of stitches. Knitted textiles provide skin comfort, low weight, and high elasticity for users[24]. Since it is a well-established traditional method, with knitting, an entire garment can be formed on one machine.

Meanwhile, knitting enables the processing of a wide variety of natural yarns and filaments. For this reason, it has been considered the most suitable method for preparing an unobtrusive, compatible fabric for a garment [98]. On the other hand, knitted structures exhibit many intermittent contacts in between the yarns, which leads to fluctuations in electrical resistivity especially in dynamic conditions [99]. Although resistance variation is undesirable for biopotential measurements as it causes larger signal artifacts, it is preferable in sensor applications such as pressure and strain monitoring.

Since conductive yarns are placed above the fabric surface, it was suggested that embroidery offers better electrode contact with the skin [22]. For the positioning of textile electrodes on garments, it can be argued that embroidery is an ideal choice for prototyping. In contrast, weaving and knitting become more useful when mass production of a smart garment is desired.

3.3.2.2. Metallic Fibers

An effective way to impart conductivity to fabrics for biopotential measurements is by adding conductive “elements” inside them. A common strategy is based on combining metallic fibers with regular yarns or fibers by following established textile manufacturing processes like knitting [100], weaving [101] or embroidery [76],[22]. Metallic fibers can be realized by creating fine metal wires [13] or through the deposition of metals on regular yarns via methods like physical vapor deposition (PVD) [102] and electrodeposition [21].

Among metals, silver provides the highest conductivity and is one of the most preferred materials due to its biocompatibility and stability [103]. In a number of different studies, silver was incorporated into fabrics made out of cotton [104], nylon [105], or polyester threads [25]. Another metal that is used for producing conductive textiles is stainless steel [106]. Likewise, copper is a good candidate due to its high electrical conductivity; however, especially in contact with water, it is prone to corrosion. To address this issue, the coating of copper surfaces with silver has been suggested [98].

Apart from the choice of metal, the type of yarn (e.g., cotton, polyester, and lycra) and fiber styles (either single filament or multifilament) along with the structure of the textile

can also affect the functionality of the electrodes. Textiles comprised of metallic yarns are relatively easy to manufacture, are flexible, and are adaptable to existing textile manufacturing environments. Nevertheless, they usually compromise the texture and natural feel of the textile, which causes discomfort especially when the percentage of metallic fiber is above a certain level [107]. This inherent trade-off between the conductivity of the textile versus the texture and wearability, therefore, requires careful balance in design.

3.3.2.3. Conductive Polymer Fibers

Another way of realizing conductive fibers is by creating polymer fibers that possess bulk conductivity. It is possible to categorize these as intrinsic conductive polymer fibers and extrinsic conductive polymer fibers [108].

Intrinsic conductive polymer fibers are produced by spinning conjugated polymers, also known as intrinsic conductive polymers (ICPs), such as polyaniline (PANI) [109], polypyrrole (PPy) [110], and poly(3,4-ethylenedioxythiophene) (PEDOT)[111]. Techniques such as melt spinning, wet spinning, and electrospinning are used to produce conductive polymer fibers. Most of the ICPs start to decay in temperatures lower than their melting point, which makes the use of melt spinning unfavorable [112]. In addition, the relative characteristics of ICPs such as poor solubility, rigid backbone structure, and low molecular weight makes them harder to electrospin [112]. To increase processability, blending with a polymer with good spinnability is suggested, but this decreases the conductivity of the polymer fibers [113]. Thus, wet spinning turns out to be the most suitable method for fiber fabrication from ICPs.

Extrinsically conductive polymers (ECPs), or conductive polymer composites, can be obtained by blending insulating polymers with conductive fillers [108]. Melt and wet spinning are common methods to produce composite polymer fibers. Wet spinning can produce fibers with better electrical and mechanical properties, whereas melt spinning is faster and free of chemical solvents [108]. As in the case of metallic fibers, conductive polymer fibers can be used to create textile electrodes with weaving, knitting, and embroidery.

Even though creating conductive fibers with electrospinning is challenging, decreasing the polymer fiber diameter down to nanometers results in a high surface area and advantageous mechanical behaviors [114]. Additionally, electrospinning is regarded as the most reliable method to create continuous polymer nanofibers [113]. It is possible to use these fibers to produce conductive nonwoven textiles, which are a good candidate for biopotential electrodes since a large contact area is a desired. Nonetheless, it is not necessary to first create conductive nanofibers and then produce a nonwoven textile to take advantage of the large surface area. It is simpler and more efficient to first fabricate a nonwoven textile with electrospinning and bestow conductivity on it with conductive fillers afterwards [115]. With this approach, researchers were able to fabricate textile electrodes and validate their performance in biopotential recordings against Ag/AgCl electrodes.

3.3.2.4. Electrodeposition

Electroless plating is a technique that involves spontaneous reactions in an aqueous solution without requiring the application of an external electric field [116], unlike electroplating, which uses an electrode current to reduce the metal cations for the coating. Electrodeposition techniques along with physical vapor deposition are the most prominent techniques to perform metal coating on non-conductive yarns and textiles.

Electroless plating on polymer fibers is an appealing choice to realize conductive fibers since it enables conductivity in all surface directions and is an acceptable way to obtain the uniform deposition of metals on complex geometries [96]. Usually, metal coating on synthetic fibers is preferred rather than natural fibers. This trend is mostly because of the low cost of synthetic yarns. The preferred metals in electroless plating are usually silver, copper, and nickel[21], [92], [117].

Despite the various fabric–metal combinations, metal-plated fabrics face durability issues when worn or washed since they can be easily peeled off from regions exposed to air or water. One of the methods that are practiced enhancing the adhesion of metals to polymeric fibers is increasing the surface roughness either with mechanical abrasion or

chemical etching [88]. Performing electroless plating followed by electroplating is an appealing coating method where electroless plating allows deposition of a more uniform coating between the starting yarn/fiber, whereas electroplating provides a larger window for thickness control [118]. To prevent wearing out of the surface coating, lamination of metal-coated polyester fabrics with a polyurethane sealing layer was also suggested [89].

3.3.2.5. Physical Vapor Deposition

PVD techniques such as thermal/e-beam evaporation and sputtering are well-established in the microelectronics process industry [119]. Similar to electrodeposition, the performance of a PVD-deposited conductive layer depends both on the nature of the textile and on the deposited layer. Its conductivity can be controlled by selection of the thin-film coating material and film thickness. So far, there have been several attempts that utilized PVD to evaporate metals and deposit thin conductive films on a variety of textiles [26], [120]. Sputtering has been used to deposit layers of silver [93],[46] and copper [4],[23] on textiles made from polyethylene terephthalate (PET) yarns and polyurethane (PU)-coated nylon fabrics.

For PVD, like other coating techniques, adhesion of the conductive materials on the surface of the fibers is critical. Removal of potential residues like oil from fiber surfaces can promote adhesion, which can be achieved by plasma cleaning or chemical treatments [121]. Metals like chromium [93] and titanium [46] have also been sputtered onto fabrics to either improve the adhesion of silver or passivate it to limit potential cytotoxicity when used in direct contact with the skin in low humidity conditions. As for the film thickness, it was shown that sputtered fibers generally require a smaller thickness of metal deposition compared to electroless-plated ones, due to the greater adhesion and smoother coating of metals via PVD [88],[102].

On the other hand, a disadvantage is that during PVD, a significant portion of the source material is lost in spots other than the desired substrate. This issue, combined with the need for dedicated equipment and a vacuum deposition environment, potentially increases the cost of the conductive textile. While there have been few attempts to produce e-textiles based on PVD, this approach is still among the less preferred techniques,

fundamentally due to the elevated cost and limited or non-trivial scalability of vacuum processing.

3.3.2.6. Dip Coating

Dip coating is one of the simplest methods to coat yarns or fabrics, and it is still used in the textile industry [122]. The process consists of the immersion of the substrate in a solution containing conductive materials such as metallic particles [123], conductive polymers [27], or carbon derivatives such as graphene [14] and carbon nanotubes (CNTs) [124]. Upon application of a conductive solution to textiles, excess material is removed [125] and a drying step, known as curing, is performed to evaporate the solvent and fixate the conductive particles on fiber surfaces. To realize a stable coating, surface properties of the textile such as wettability and hydrophilicity are important [125]. Care should also be taken to limit the drying/curing temperatures to avoid potential damage to the textile [126].

Conductive solutions or pastes are the only feasible way to utilize graphene/CNTs in textile coating. Although multiple techniques such as chemical vapor deposition (CVD), mechanical exfoliation, epitaxial growth on silicon carbide, and chemical reduction of graphene oxide (GO) exist for preparing graphene [127], the latter approach (i.e., chemical reduction) is the most suitable and applicable for textile surfaces due to low-temperature processing and scalability [128]. In graphene-coated textile preparation, the desired piece of textile is dipped in a GO solution, and subsequent drying provides fixation on fiber surfaces. As for post-processing, a chemical reduction procedure is performed to convert GO flakes into graphene, allowing electrical conductivity to be imparted [47],[14]. Carbon nanotube (CNT) powders have also been used to create conductive fabrics [129]. For instance, textile electrodes were fabricated by cladding cotton fabrics with multi-walled CNTs (MWNT). To ensure their adhesion, a conductive paste made from tapioca starch and MWNT powder was applied to the surface and cured afterward [130]. Another aspect of wearable monitoring was looked into with the creation of conductive cotton yarns to use in biosignal transmission [124]. Regular cotton yarns became conductive with dipping in a single-walled carbon nanotube () solution and drying afterward, which fixated SWNTs to cotton microfibrils.

Regarding the biocompatibility of CNTs, while there is some concern regarding their cytotoxicity, the purity of the carbon nanotube (i.e., elimination of trace metals such as iron that get incorporated into CNTs during manufacturing) has been shown to be a critical factor, especially for the case of dermal administration and exposure to CNTs [131]. Arguably, with better control of purity, it may be possible to reduce or eliminate the potential toxicity of CNTs when used as part of conductive textile electrodes placed in direct contact with the skin. Graphene, on the other hand, has been shown to have minimal effects on skin as long as the concentration and exposure duration is moderate [132].

The simple and scalable nature of dip-coating allows the manufacturing of rolls of conductive fabrics with lower fabrication cost, and after cutting and sewing of the desired patch, it is also possible to attach textile electrodes onto an existing garment[20].

3.3.2.7. Printing

Printing techniques such as ink-jet and screen printing are widely used to create conductive patterns on textile substrates, and these are already used on a large scale to print decals/images onto textiles [133]. Some advantages of printing techniques include: (a) site-specific, localized, and direct deposition of conductive materials on finished roll-to-roll (R2R) fabrication textiles; (b) reduced consumption of chemicals/inks; (c) ability for adaptation to both desktop scale R&D and commercial manufacturing environments with the potential to be combined into or allow further reduction of e-textile production costs.

Screen printing uses a fine mesh or stencil with openings to enable preferential passage of viscous, conductive inks/pastes, while ink-jet printing is a well-known maskless technology that can interface with numerous ink–substrate combinations to address both daily applications as well as advanced areas such as biomolecular patterning [134]. In a single pass, screen printing can deliver higher amounts of ink compared to ink-jet printing. Therefore, screen printing requires fewer printing cycles to achieve a stable conductive pattern on textile surfaces. Another aspect is regarding the contact and non-

contact nature of the printings. Applied pressure in screen printing promotes adhesion, penetration of the ink to the substrate, and facilitates the formation of connected patterns. Conversely, non-contact ink-jet printing relies on the spread of the ink to achieve the merging of successive ink droplets and form electrically-connected structures, which requires careful engineering of the ink diffusion and printing process, especially on rough textiles where yarn-to-yarn spacing may be on the order of tens of microns [90]. Inkjet printing's flexibility in pattern creation and available materials makes it versatile for e-textile research [135]. On the other hand, screen printing seems to be ahead of ink-jet printing for the creation of e-textiles for consumer products. It is faster since it allows the transfer of larger amounts of ink at one time, and it is a mature technology already used in industry, which makes screen printing a cheaper alternative.

Printing technique, nonetheless, is not the only consideration for achieving optimal conductive pattern transfer. Ink properties such as viscosity and curing temperature, and surface properties such as surface roughness and surface energy, affect the accuracy of pattern transfer [136]. Using an ink with high enough viscosity is important to contain the ink on the desirable pattern after deposition. This calls for the addition of binders to engineer the ink viscosity, which often affect the conductivity negatively.

It is not easy to control the surface properties of woven fabrics; the resolution achievable by printing on them depends on both the yarn diameter and inter-yarn distance. As an alternative, the surface texture, density, porosity, and thickness of nonwoven fabrics can be controlled during fabrication. They are also cheaper and faster to fabricate, which makes them better substrates on which to print [136]. Nevertheless, woven textiles are known to be more flexible and breathable than nonwoven ones, which makes them more comfortable to wear. Moreover, it was suggested that the creation of a high surface energy interface layer on top of the fabric can provide a desired substrate on which to print, while conserving the comfortable wear of the woven fabrics [7]. The extra interface layer is not expected to affect comfort since it can also be printed on only the desired areas, such as electrodes and their interconnections.

Metallic inks/pastes can be produced by using metallic nanoparticles, metallo-organic complexes, or metallic salts as precursors [137]. Even though there are commercial metallic inks (mostly silver-based), their curing temperatures should be lowered to be

compatible with textile substrates, and their cost should be decreased so that they can be used in the mass fabrication of textile electrodes. Conductive polymers are also studied to create alternative conductive solutions. Their conductivity is typically lower than their metallic counterparts, but their adhesion and mechanical stability are better, and they do not usually require post-treatment steps. To this end, poly(3,4-ethylenedioxythiophene) polystyrene sulfonate (PEDOT:PSS)-based solutions are regarded as the most promising material to enter the market, due to their flexible processing and durable electrical conductivity [138], [139]. Dispersions of graphene or CNTs can also be used in printing to create conductive patterns [29], [140]. The effect of pretreating the fabric to increase its printability was also shown with ink-jet printing a hydrophobic layer prior to application of GO solution [29]. This helped to improve the continuity of the conductive layer by three orders of magnitude compared with untreated coating.

3.3.2.8. Chemical Solution/Vapor Polymerization

Vapor deposition, electrochemical deposition, and in situ solution polymerizations are techniques that allow the formation and deposition of intrinsically conductive polymers in a single step.

Vapor deposition allows uniform coating for any surface morphology or roughness, and coating can be thin enough to not change the mechanical properties of the fibers. Two main ingredients used in vapor polymerization are conjugated monomers and iron salts as oxidant agents [141]. They are used to create conductive polymers in two distinct ways: impregnation of the oxidant solvent to textile with dipping/printing followed by monomer vapor feeding, and the simultaneous application of both the oxidant and conjugated monomer vapor. A closed chamber is required for the application of vapors. This process, however, is not solvent-free since oxidant residues need to be rinsed after vapor deposition, and they require vapor chambers, which limit the scalability of the process. Nonetheless, with the advancements made in the past, the textile industry recently started to adopt this technique [141] because vapor-deposited films inherently show wash and wear resistance, as opposed to the need for binders in the dip-coating method. Additionally, vapor-deposited textiles show higher conductivity compared to the conductive textiles created with commercial polymer inks [141]. For instance, coating of

polyester fabrics with PEDOT by vapor polymerization revealed a sheet conductivity as low as $10 \Omega/\text{sq}$, which is claimed to be among the best in any kind of synthesis of PEDOT and its dispersions [97].

Polymerization can also be done by placing the textile substrate in a solution containing the monomer and adding an oxidant to the solution, which starts the deposition; this is called in situ solution polymerization. Even though it is a relatively simple process, polymerization is hard to control. It is possible to degrade the textile substrate with acidic reaction conditions, which can harm the mechanical characteristics of the textile [141].

Electrochemical polymerization happens with an application of varying voltage on an electrode in a solution including a monomer and electrolyte salt; polymer coating occurs on the electrode. Textile fibers are natural insulators, and to be able to use electrochemical deposition for coating, it is first necessary to create a conductive seed layer on the fibers with other polymer deposition techniques. Not surprisingly, the final morphology of the coating is mainly determined by the previously coated seed layer. Electrochemical polymerization can be regarded as a technique to increase the thickness of the polymer coating in a more controllable fashion [142]. For example, textile electrodes were created by coating PPy on cotton fabrics via initial in situ solution polymerization followed by electrochemical polymerization [94].

Like the rest of the fabrication methods, the choice of technique for conductive polymer coating boils down to a trade-off between desired quality and cost. Vapor polymerization is an apparent example, which promises the best quality with possibly the highest cost. Optimization can be achieved by improving existing techniques or using them in combination, which requires knowledge of the whole palette of techniques.

4. PREPARATION OF GRAPHENE COATED TEXTILE AND GRAPHENE ARMBAND

4.1. Textile Synthesis

Graphene has been a great deal of attention in recent years because of its unique electrical and structural properties. It has a (2D) single layer structure of sp^2 bonded carbon atoms similar to the Graphene honeycomb pattern. These atoms are connected with the neighbour atoms at a length of 0.142 nm [143]. rGO synthesis steps are shown in figure 4.1. Owing to these unique properties, graphene and its derivatives have been applied in many fields from biosensor to nanoelectronic devices [144]–[148].

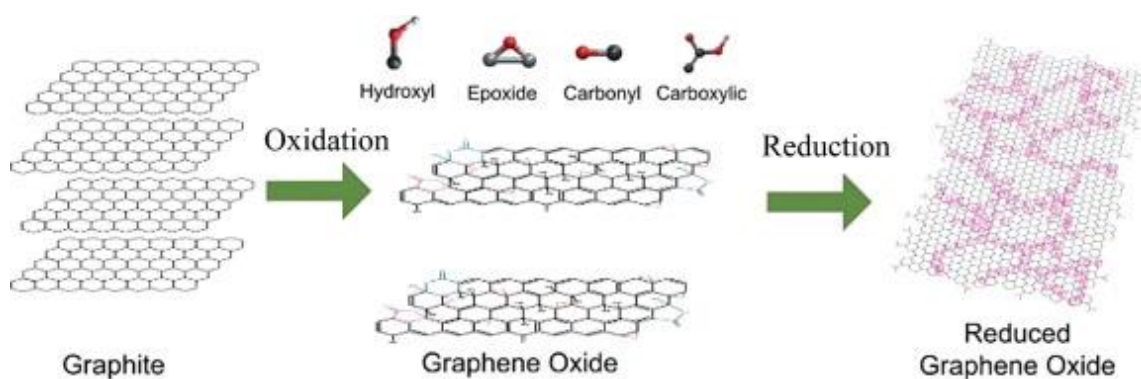


Figure 4.1 RGO synthesis steps from oxidation to reduction[149]

In this study, flexible, low-cost and wearable, graphene deposited textile electrodes were produced as an alternative to commercial Ag/AgCl electrodes. Graphene oxide (GO) was synthesized based on the modified Hummer's method, and nylon textiles were dip-coated homogeneously with GO. Upon drying, stable GO-coated textiles were obtained, after a

reduction reaction was performed to form conformal graphene coatings on textiles. This chemical reduction process disrupts the sp^2 structure of graphite, making the epoxide and hydroxyl groups as hydrophilic because they bind to the basal planes and functional groups such as carbonyl and carboxyl at the edge. Also, it includes reducing agent as chemical treatment [150], [151]. The quality of properties and potential application areas of the graphene produced may vary by the selected reduction process [152]–[156]. After reduction, textiles were cleaned by immersing it into de-ionized (DI) water and dried in a vacuum oven. Schematic summary of graphene textile coating processes is shown in Fig. 4.2.

The reduced graphene oxide (rGO) includes many of the residual functional groups leading to increase the intermediate layer spacing while reducing the interaction effects of van der Waals force between the graphene layers. Especially, nylon was selected in this study due to its minimum surface roughness. Conductivity measurements showed that the resistance of textiles was between $3\text{ k}\Omega$ to $5\text{ k}\Omega$.

During the conversion of graphene oxide to graphene, there is a noticeable change in the textile colour from brown to black. It also results in the hydrophobicity of the materials as a result of the removal of oxygen-containing groups. The development in the current conductivity of the graphene materials with the increase of the C / O ratio indicates the effectiveness of the reduction process. Although the reduced graphene oxide formed after reducing treatment can maintain its layered structure, it is lighter than graphite due to the loss of electronic conjugate caused by oxidation [149]. The changes in chemical structure during the reduction progress of GO were observed in the Raman spectrum as shown in figure 4.3.

To handle the graphene textiles and for rapid testing, the ECG lead cables were attached onto flexible textile surfaces by snap-on connectors. Three times immersing of the textiles in water did not cause significant resistance change of graphene textile surface.

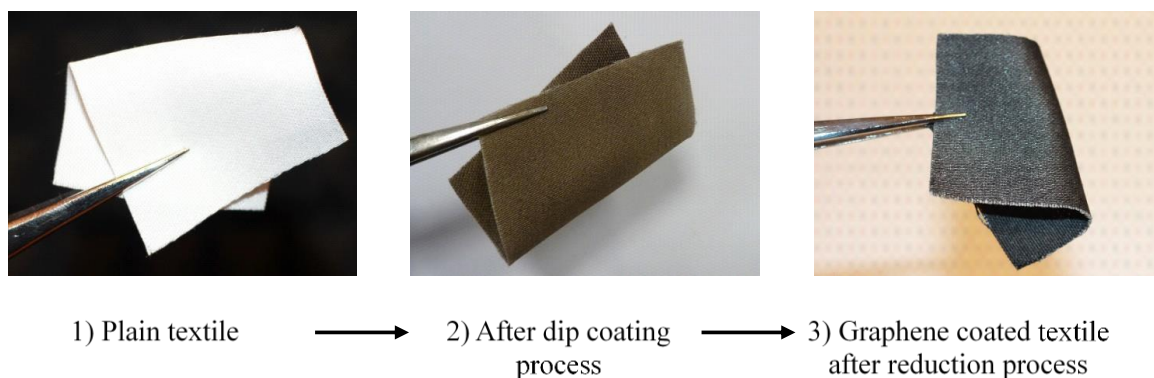


Figure 4.2 Schematic summary of graphene textile coating processes

Figure 4.3 shows the Raman spectra of reduced GO electrodes on arm bands. Graphene-based materials have two characteristic Raman shifts around 1343 cm^{-1} and 1594 cm^{-1} , which are called as D and G-bands respectively. The G-band is linked with sp^2 -hybridization of carbon atoms through 2D hexagonal plane while D-band is associated C-C sp^2 hybridized between the hexagonal flakes. Increment in the number of C-C sp^2 hybridization is connected to deformation of the bonds between hexagonal flakes, which means forming of reduced GO. An increase of the number of deforming results in increasing of I_D/I_G ratio. On the other hand, G peak is the crystalline graphite. Therefore, the intensity proportion between D (I_D) and G-band (I_G) illustrates the formation of defects in graphene layers. The higher ratio of the ratio is linked to reduced graphene oxide condition. While the I_D/I_G ratio was 0.89 for the GO, the value increased to 1.32 for the rGO on textile. Also, as it is clearly seen in the scanning electron microscope (SEM) images in the figure 4.4, the fibers of the textiles having a fibrous structure were homogeneously coated with graphene and the core of the fibers were not coated.

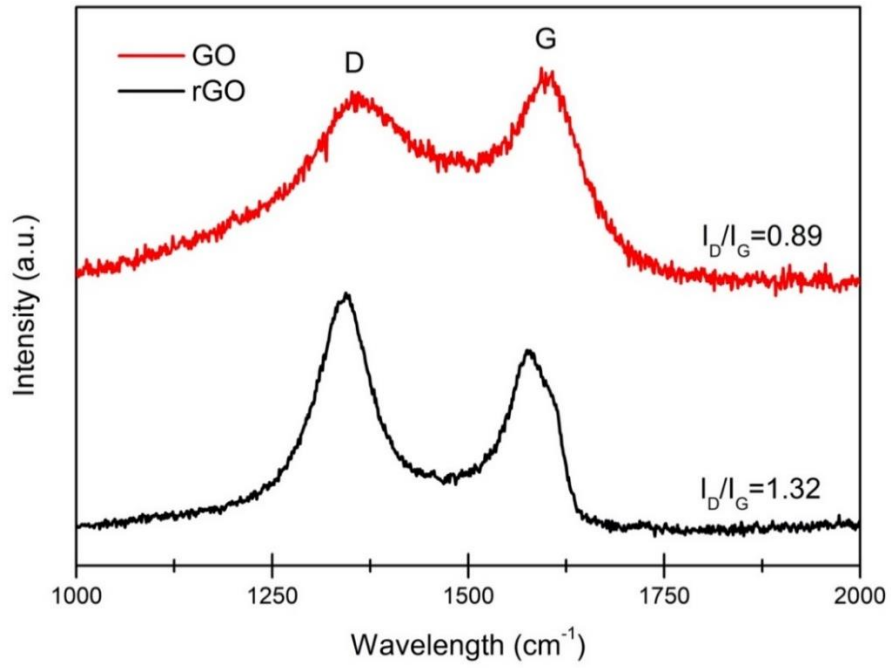


Figure 4.3 Raman Spectrum Analysis for Graphene Electrode

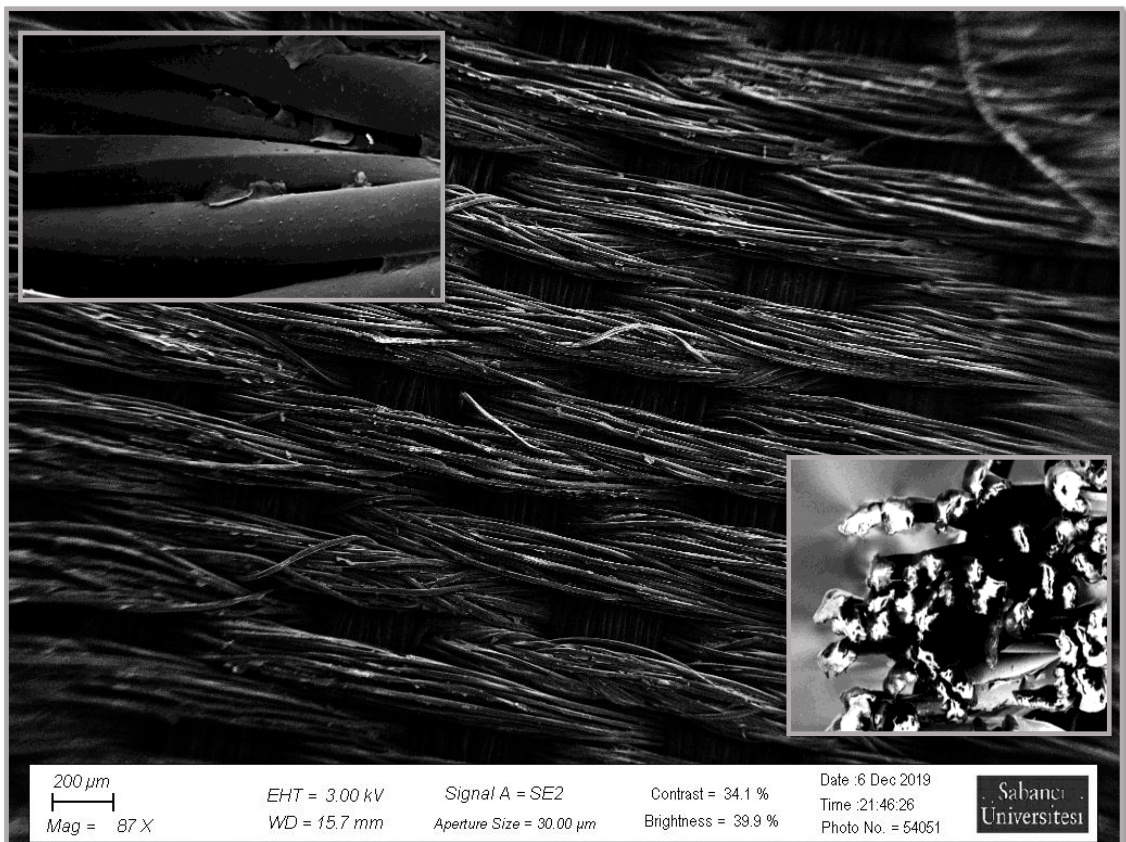


Figure 4.4 SEM images of graphene coated textile electrodes

4.2. Direct Patterning of Garments by Spray/Stencil Printing

Spray/stencil printing processes have been used to produce textile for human bio-potential monitoring applications. Stencil printing, which is widely used in the textile industry, is a suitable technique for making conductive electrodes. Conductive textiles can be formed by using a stencil printing technique as well as the dip-coating technique. Three electrodes are located on a single armband to receive and interpret ECG signals. The previous section mentioned the construction of three individually produced electrodes. This section explains how high conductive graphene-coated garment that make them favourable for health monitoring systems, is produced by using stencil printing technique of three electrodes directly on single armband. The armband did not require the integration of electrodes into the textile. Since they provide electrical contact with the skin without having to sit tight and they are also bendable and provide more comfort, they are more favourable to collect ESG signals. Thus, a more comfortable and breathable garment for obtaining an ECG signal is obtained.

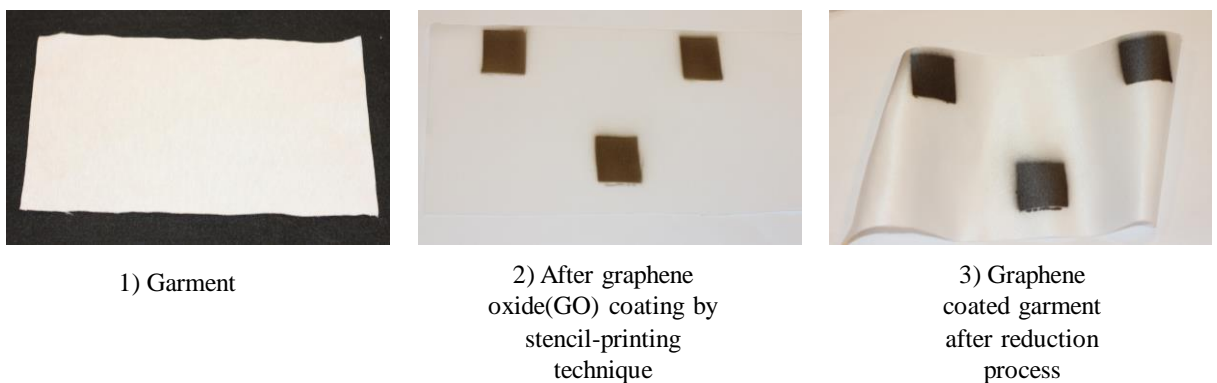


Figure 4.5 Processes of graphene armband preparation

The stencil can ease of printing to the electrodes at the desired dimensions. By using a stencil process, the specially selected regions on the textile were imprinted by GO which is synthesized by Hummer method. Subsequently, reduction of deposited GO was

achieved by chemical reactions and treatments. Then, the textile was washed by immersing it into DI (water) to recover from the remaining chemical wastes and impurities, followed by drying in a vacuum oven at 80 degrees. Preparation process of graphene garment is shown in figure 4.5. Resistance measurements, skin-electrode impedance values, Raman spectral (figure 4.6) and SEM (figure 4.7.) results were reported. Raman spectral analysis was performed from the regions coated with GO on the garment and from the same regions which became reduced GO after chemical treatment. Graphene-based materials have two characteristic Raman shifts around x and y, referred to as bands D and G, respectively. It was mentioned in the previous section that the reduced GO value is relevant to the I_D / I_G ratio. Thus, the density ratio between D (I_D) and G-band (I_G) indicates defect formation in the graphene layers. The high proportion of the ratio is due to reduced graphene oxide conditions. While the I_D / I_G ratio for GO was 0.89, the value for rGO on textile was found to be 1.38. According to SEM images, plain wave knitted textile electrodes were coated more homogenously, and reduction processes were applied at the same time.

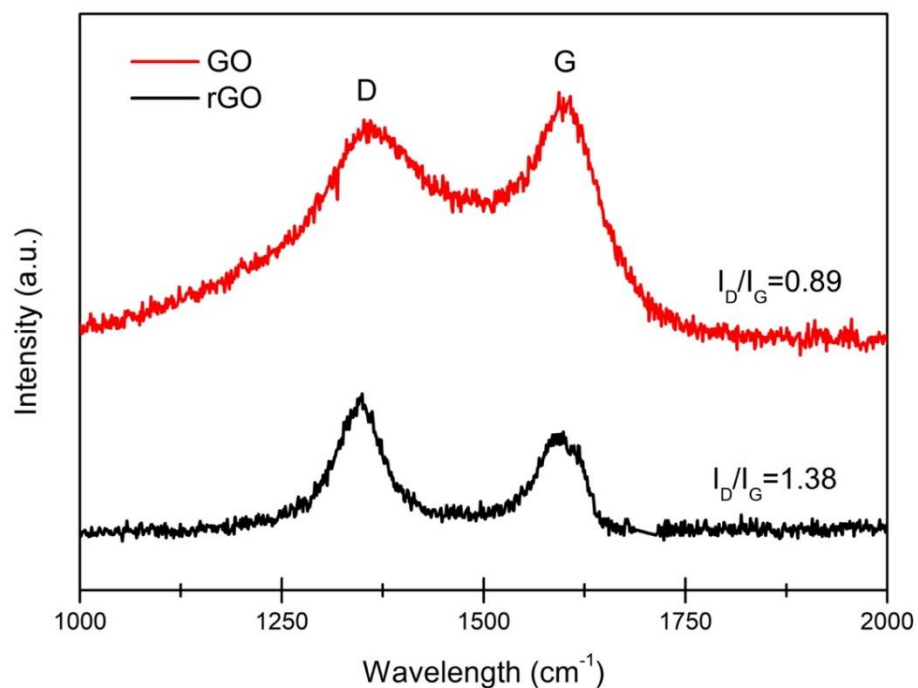


Figure 4.6 Raman spectra results of graphene coated armband and graphene oxide(GO) coated armband

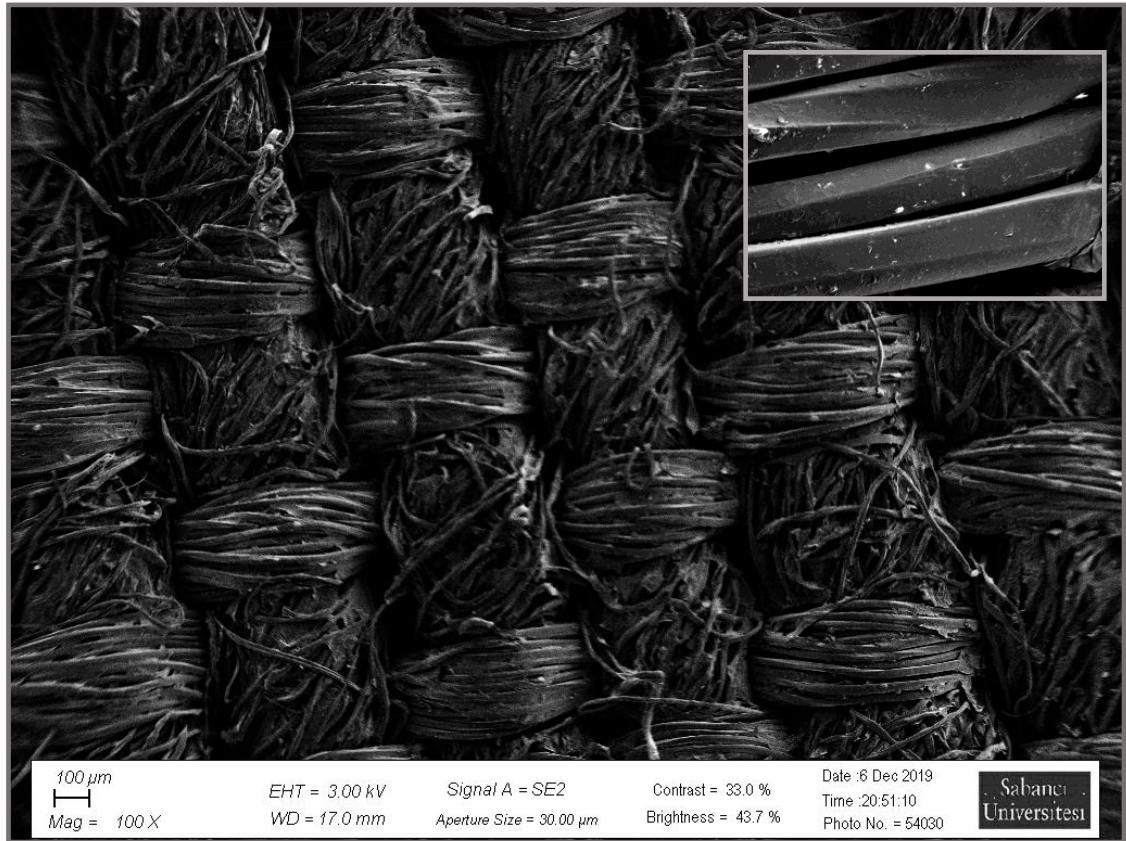


Figure 4.7 SEM images of graphene armband

4.3. ECG Acquisition Circuitry

Typically, the amplitude of the ECG signals from surface electrodes varies between 0.1–5 mV while the dominant frequency range lies in between 0.5–40 Hz. In wearable applications, however, ECG signals are further distorted due to motion artifacts, noise and coupling resulting from closely-placed electrodes, and interference due to other biopotential signals such as electromyography (EMG), which make accurate replication of the electrocardiogram a non-trivial task. To detect the electrocardiogram and prevent signal deviation, analog filtering was performed below 40 Hz. Figure 4.8 depicts the system-level block diagram of the ECG acquisition circuit for ECG recording from a single arm with minimum number of electrodes and components. In order to receive a smooth and noiseless ECG signal, it is imperative to filter the EMG signals, noise signals from motion artifacts, powerline noise (50 Hz) and other sources. One of the most necessary conditions to obtain satisfying ECG signal acquisition data is to use high-

quality electrodes. The signal acquisition system consists of a combination of typical signal receiving units, high-efficiency hardware and the required software. The system has been designed in such a way that it provides flexibility to the electrodes and a quality wireless system with a suitable cost. A digital signal processing (DSP) algorithm was used in all the filtering stages.

The block diagram of the prototype system prepared for ECG signal reception and signal processing are shown in figure 4.8, and the characteristics of the components used in the system are shown in table 4.1. At the analog front-end, the circuit obtains its surface potentials via graphene textile electrodes and after denoising.

It is then sent to the microcontroller to digitize the analog signals. Digitally converted signals are transmitted via a wireless connection to the PC using LabVIEW® (National Instruments, USA) and MATLAB® platforms. Thanks to the graphical user interface (GUI), the real-time data can be stored and tracked. The circuit first has second and fourth-order Butterworth high-pass and lowpass filters with cut-off frequencies, commonly, depending on the Sallen-Key topology in the preprocessing stage to reduce noise. The selected instrumentation amplifiers (INA122, Texas Instruments, USA) and op-amps (OPA2365, Texas Instruments, USA) are suitable for the battery-operated and portable ECG signal acquisition system. A voltage divider (MAX5421, Maxim, USA) was used to adjust the phase gain of the post-amplification level. The system has been realized wirelessly via Bluetooth.

As a power source, lithium-ion / polymer battery has 3.7 V and 500mAh specialities were used to integrate it conveniently into a wearable system. As the battery charge management circuitry and DC-DC boost charge converter MCP73831 (Microchip, USA) and TPS61090 (Texas Instruments, USA) were preferred in orderly. A rail-splitter (TLE2426, Texas Instruments, USA) with a voltage divider with a buffer circuit was applied to avoid unbalanced occurrences when dividing the regulated 5 V. In order to provide computer data flow, Bluetooth was designed using HC06 module, and the data received with a GUI designed in LabVIEW was followed. The scope of the Bluetooth prototype system is 5 meters, and the battery life is 4 hours.

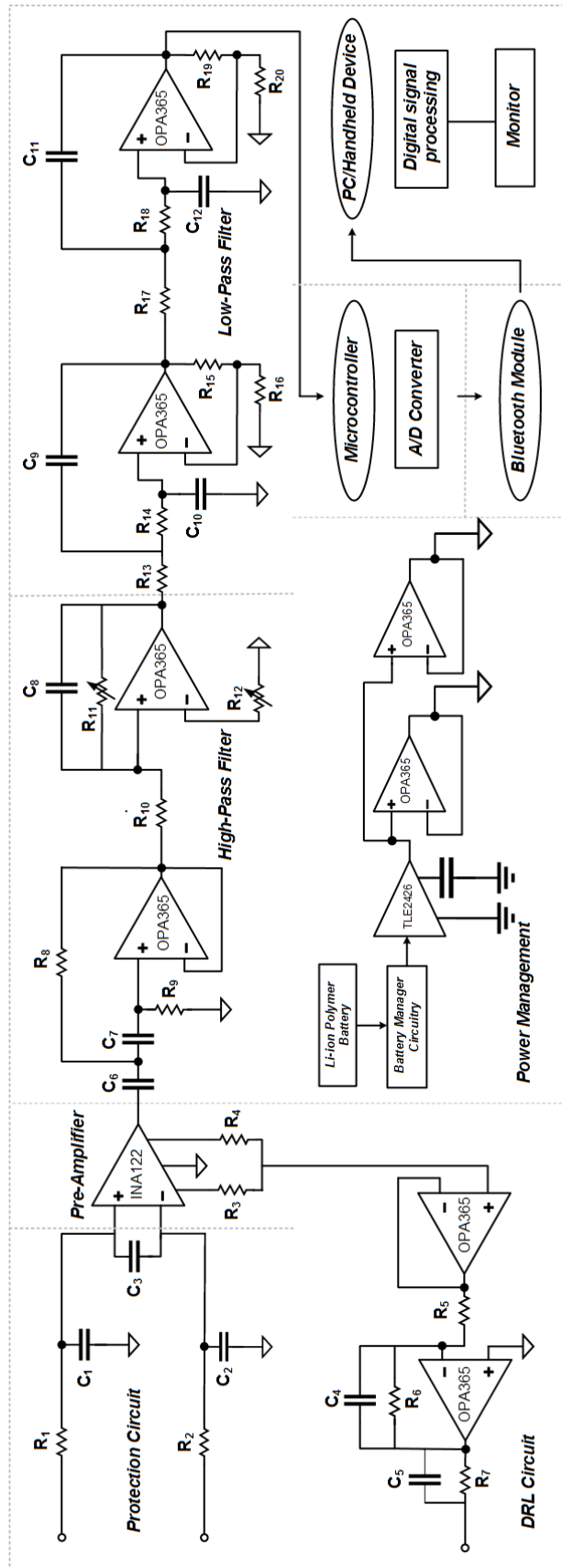


Figure 4.8 The hardware level schematic of the analog section of the signal conditioning unit and block diagram of the developed ECG system for real-time monitoring and recording

Table 4. 1 Component sections and specifications for signal acquisition system

Sections	Specifications
Protection Circuitry	$R_1, R_2: 1k\Omega,$ $C_1, C_2: 1nF, C_3: 100nF$
Pre-amplifier	$R_3, R_4: 20k\Omega$
DRL	$R_5: 10k\Omega, R_6, R_7: 390k\Omega,$ $C_4: 1\mu F, C_5: 270nF$
High-Pass Filter	$R_8, R_9: 36k\Omega, R_{10}: 4.7k\Omega, R_{11}, R_{12}$ (potentiometer): $1k\Omega,$ $C_6, C_7: 1\mu F, C_8: 1nF$
Low-Pass Filter	$R_{13}, R_{14}: 10k\Omega, R_{15}: 330k\Omega, R_{16}, R_{17}: 0\Omega, R_{18}: 330k\Omega, R_{19}: 390k\Omega, R_{20}: 0\Omega,$ $C_9, C_{11}: 1\mu F, C_{10}, C_{12}: 270nF$

4.4. Wearable Prototype

The heart muscles (i.e. myocardium muscles) are contracted due to the potential change in the human heart. The potential difference results in circulating currents around the body which can be detected to form the electrocardiogram. In literature [157] ECG signals are collected to produce Einthoven's Triangle by locating two electrodes on both arms and the third one on the right leg as a reference electrode. However, it is possible to get the signals by putting three electrodes on a single-arm [158], [159].

To realize single-arm, ECG measurement based on our “all textile-approach”, an elastic armband with embedded graphene textile electrodes was constructed as shown in figure 4.9. Variation in electrode locations was observed to result in different signal patterns, and graphene textiles placed in a triangular configuration with ~ 6 cm center to center spacing were found to display the best ECG waveforms.

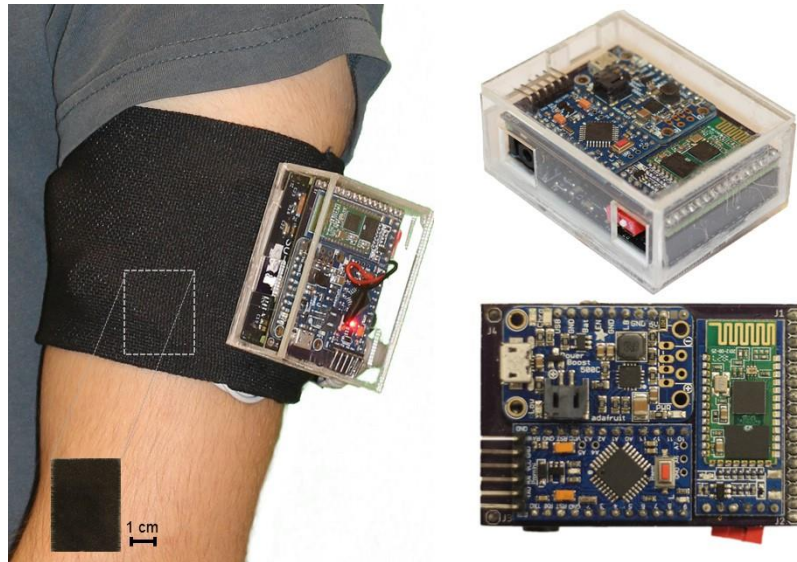


Figure 4.9 Integrated system of graphene armband with ECG acquisition circuitry

The main drawback of the screen and stencil-printed manufacturing method is that it has poor planar electronic compatibility with fiber-structured textile electrodes and is not reusable compared to conventional Ag / AgCl electrodes. The processes for forming these systems are textile compatible, relatively low cost and suitable for a production line.

All electrodes are placed to the skin at the same time, and these garments can be reused. The location of electrodes is determined whilst the manufacturing process, which saves time, but improves accuracy. For this reason, the electrode gap needs to be kept constant. A new template can be produced using 3D printing or injection molding, which makes it easier to produce and develop smart textiles.

In order to detect the ECG signals received from different points on the upper side of the arm, graphene electrodes of 2.5 * 3 cm dimensions were pressed in the three regions of the garment, and the connections of the cables with the flexible adhesive foils sanded between the metallic snap fasteners provided as shown in Figure 4.10. In order to achieve the desired bio-potentials, the electrodes must be placed on the skin surface and have firm contact.

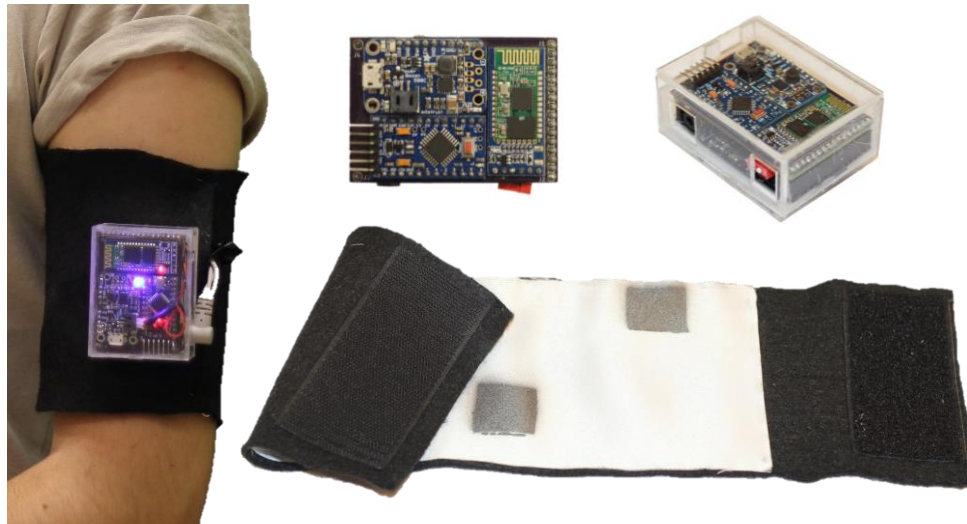


Figure 4.10 Integrated system of graphene garment with ECG acquisition circuitry

4.5. Skin Electrode Impedance

Skin-electrode impedance value is one of the crucial performance criteria to understand its suitability of the electrodes in a wearable ECG system. The skin-electrode impedance characteristic, which is one of the parameters determining the quality of the received signal, should be small and stable. The impedance of the graphene-coated textile electrodes were characterized, as shown in previous studies [14],[160],[161],[162]. The impedance of graphene textile electrodes and Ag/AgCl electrodes were measured by three participants who have different skin types; normal skin, dry skin and oily skin. The three electrodes were placed on the inside of the arm 5 cm away from the wrist. The produced current was applied to the skin by the placed electrodes. The reference electrode was held at ground potential.

Ag / AgCl electrodes were used at the edges of the reference and counter electrode. The performed electrodes were placed close to Ag / AgCl or graphene-coated textile electrode according to the type of the electrode in the device. The impedance of Ag / AgCl electrode for oily skin in the frequency range 1Hz to 1 kHz varied between 74 Kohm and 16 Kohm, while the impedance value of graphene-coated textile electrode ranged from 67 Kohm to 16 Kohm. These were preferable for a commercial electrode, that a significant difference

between the Ag / AgCl and the graphene electrode was not detected, as shown in figure 4.11. Especially the graphene textile electrode has a better impedance characteristic compared to the Ag/AgCl electrode.

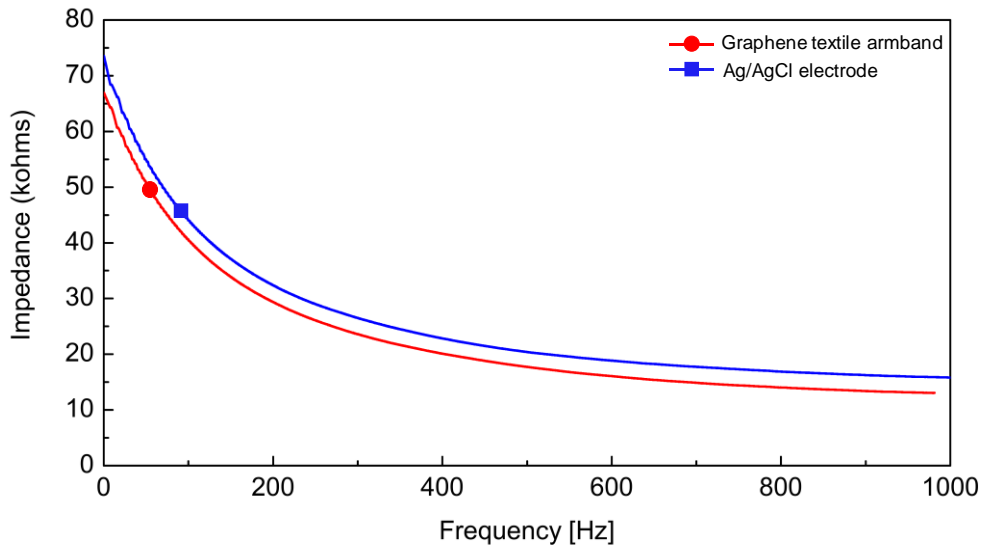


Figure 4 11 Comparison skin electrode impedance values with Ag/AgCl electrode and graphene textile armband.

Also, it was observed that the conductivity values of the samples taken from different regions of the textile after different coating lengths were between 12.4 S/cm and 26.6 S/cm as shown in the graph. The best result was the value of the sample cut from the center of the textile to a length of 5 cm.

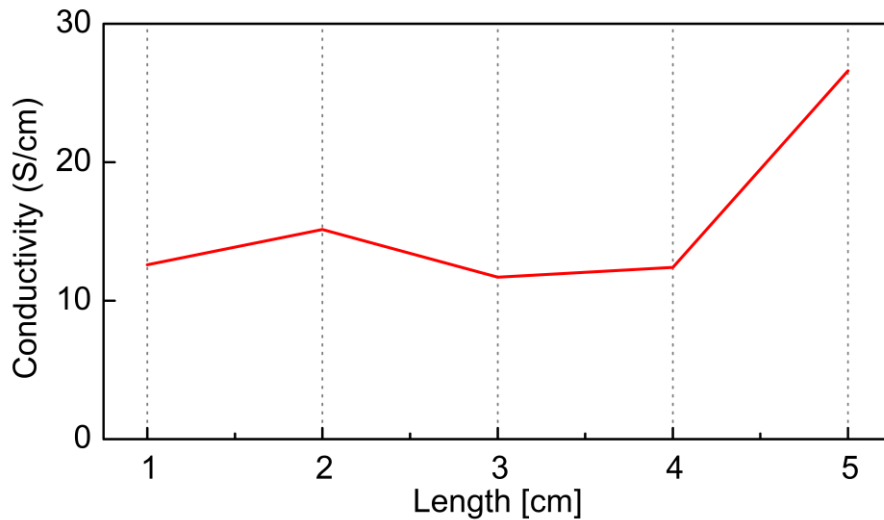


Figure 4.12 Conductivity measurement results for different length and different part from graphene coated textile.

5. RESULTS AND DISCUSSION

The wearable smart clothes are popular since it is possible to make a smart outfit monitoring biopotential signal in a comfortable and convenient way. Textile integrated biomedical sensors such as Ag / AgCl electrodes, which are used in clinics to provide information to the users about their condition, can achieve long-term bio-potential signals monitoring. This section shows our report of a complete wearable system where long time heart signal can be monitored by taking ECG signals from a single arm. the armband produced directly by coating conductive textiles as three regions onto a single textile. Electrodes are coated and manufactured using different techniques. The ECG's Bluetooth module, as well as the front-end circuitry, are integrated into a PCB for compact mounting and information transfer over the upper arm support.

5.1. Single Arm Band with Graphene Electrode

Each measurement was made using three electrodes in a differential measurement configuration, and the data was transmitted wirelessly to a computer for analysis, and signals were observed through designed graphical user interface. Both electrodes were fed through the designed ECG circuit so that samples could be compared without bias. This was accomplished by collecting and recording ECG signals wirelessly from the arm of nine subjects using the Ag / AgCl and graphene electrodes which is close to the Ag / AgCl electrodes on the subjects' armband. To determine the quality of physiological recordings using the developed electrodes, we have reported similarities and correlation rates between the signals obtained from them and the signals recorded at the same time using Ag / AgCl electrodes. The presented results show that graphene electrodes receive

bio-potential signals competing with conventional methods and can also be obtained from a single arm. The wireless transmission interface combined with the armband makes it ideal for early detection of cardiac events and long-term monitoring applications.

The ECG signals collected by Ag / AgCl electrodes and collected at approximately the same time by fabricated graphene textile electrodes were compared (3 M Red Dot™, 2560) in three different steps to correlate the accuracy of ECG signal received from a single arm. By fixing the three electrodes integrated on the armband to the single-armband, the signal reception was carried out for three different situations, sitting, standing and walking. The two electrodes represent lead points, while the third electrode was designated as the reference electrode. Graphene coated textile electrodes were used for receiving and recording. In this study, ECG recordings were obtained from the nine volunteer participants aged 22-52 years (mean 31). Although none of the nine participants had heart problems, they were asked to be comfortable throughout the ECG recordings so that the EMG signals did not interfere with the ECG signals. Heart signals were recorded from one participant for 300 seconds for the same conditions with the other eight participants as shown in figure 5.1. In addition, Heart signals were received from the eight participants during sitting, standing, and walking, each lasting 15 seconds as shown in figure 5.2.

The MATLAB correlation function was used to measure the correlation between the signals received with graphene textile electrodes and the conventional electrodes. The correlation was observed by the GUI based on LabVIEW. The correlation values of the signals recorded from the eight participants were max 96% and min 84% for sitting signals, max 98% and min 76% for standing signals, and max 93% and min 70% for walking signals. Detailed correlation values are shown in Table 5.1. For detailed comparison and interpretation of 15 seconds, ECG signals of both electrodes for each participant are shown in figure 5.2. Signal processing features were exploited to interpret the ECG waveform. P wave, QRS complex and T wave can be easily detected using the parameters of ECG morphology. The R peaks, which are one of the most critical parameters in calculating heart rate or bpm value, are obvious to detect due to their large amplitude. Heart rates can be determined from a distance between the two successive R-R peaks that the change in the distance within these parameters can also be interpreted as heart-related problems. The bpm was obtained by the detection of R-R peaks in the ECG

signals taken from nine subjects at different positions. The method developed by Lee et al. was used to complete the heart rate [12]. The R peak can be separated from the baseline corresponding to 70% of the recorded ECG signal. The BPM value would also be monitored from the signal monitoring system that we have developed. It was observed that the bpm values obtained by the ECG signal monitoring device could measure bpm in clinics practice, as shown in figure 5.4 and in table 5.2. In ECG biopotential signal measurements, the placement of electrodes and the quality of the electrodes are important indicators for the characteristics of the obtained signals. It was observed that the signals received with graphene electrodes during signal reception were less noisy and had ECG waves (P-QRS-T). It is complicated to obtain clear ECG signals due to the interference of EMG signals and noise signals during walking. Acquired signals by walking caused motion artifacts in ECG signals. However, the high correlation rates of integrated graphene electrodes with single armband have shown that it can be used in daily life.

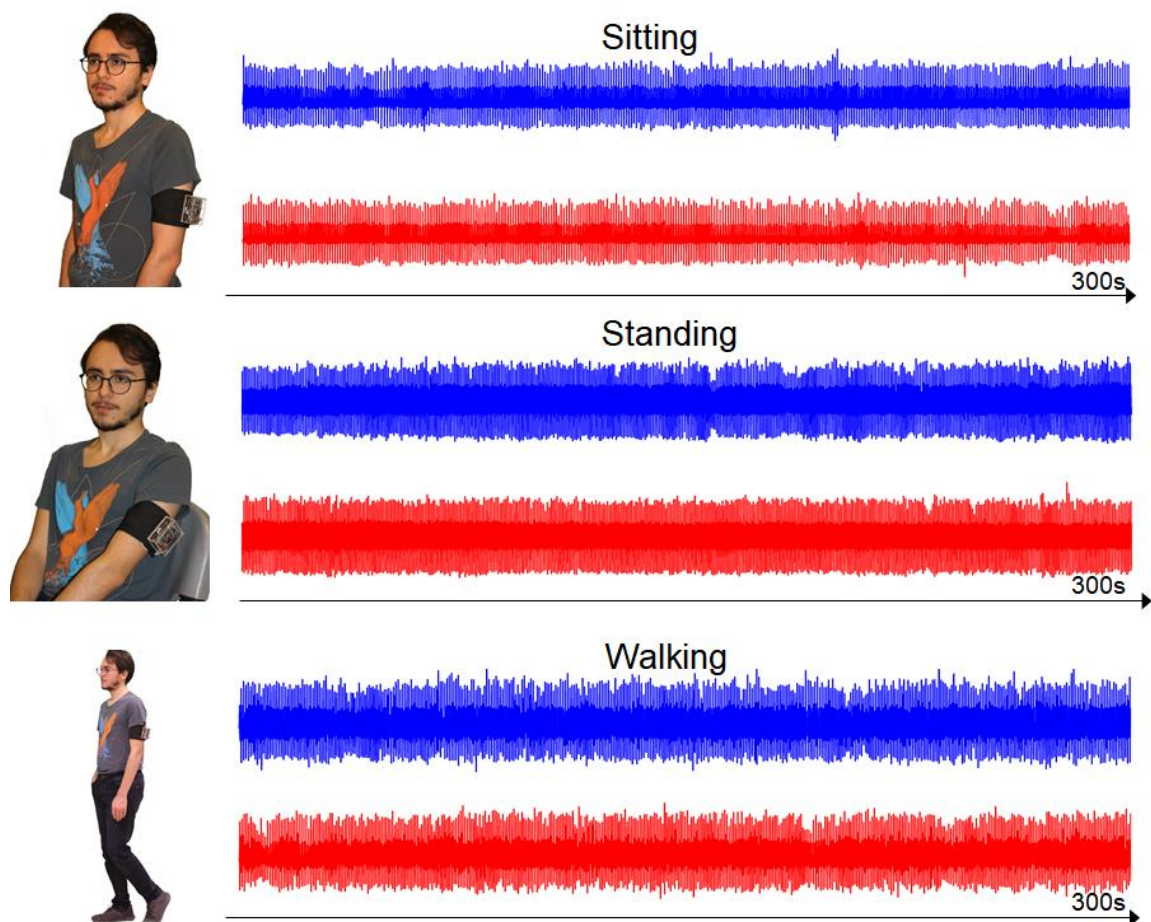


Figure 5.1 Experimental setup showing the simultaneous acquisition of ECG from the subject with graphene textile armband and plot of the recorded signals for three cases are sitting, standing and walking for 300 seconds.

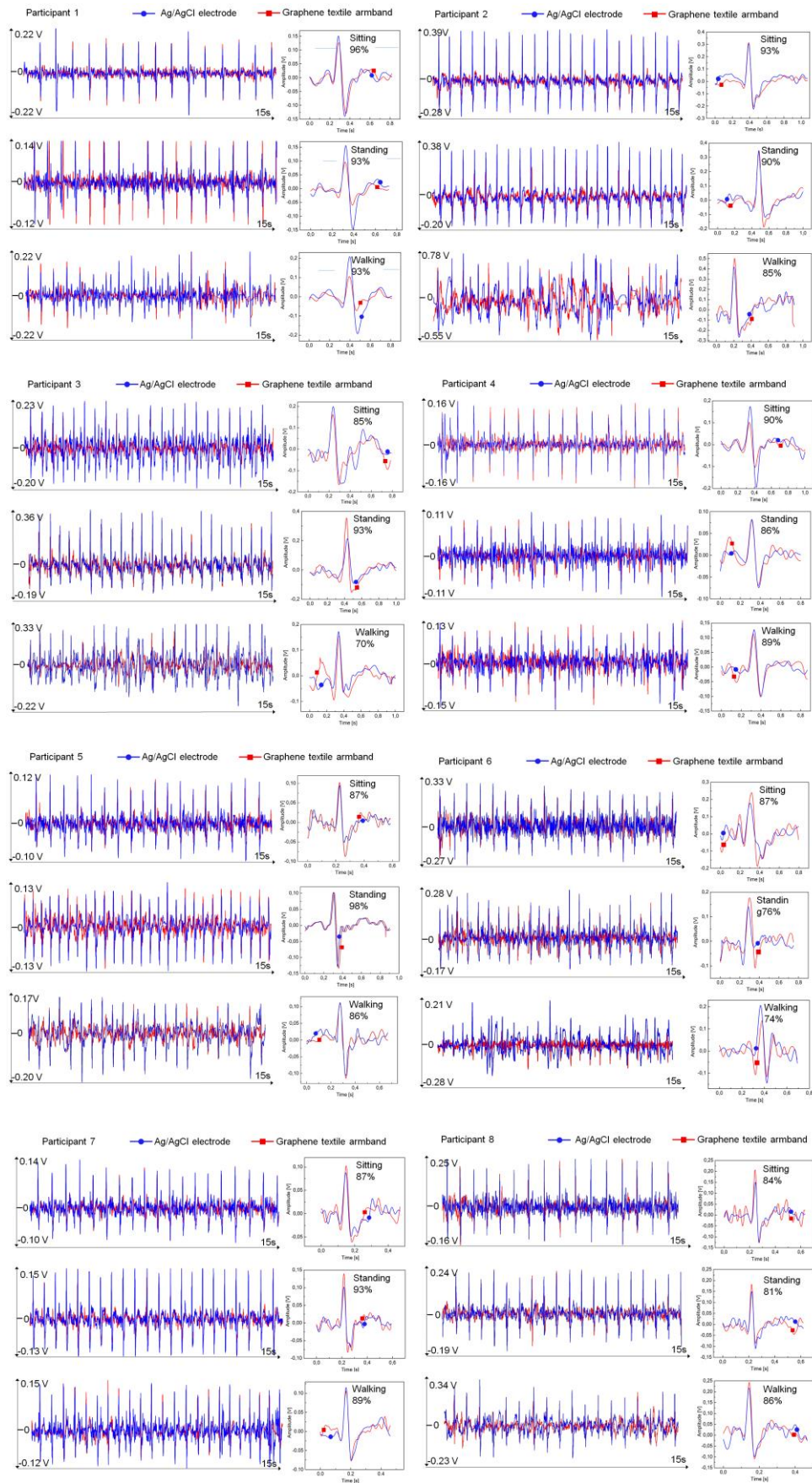


Figure 5.2 Graphs of ECG recordings obtained using graphene textile and Ag/AgCl electrodes that displayed the highest correlation among the 3 cases on 8 different participants



Figure 5.3 Some of participants.

Table 5. 1 Correlation Coefficients Between Signals Obtained with Graphene Textile and Ag/AgCl Electrodes

Subject	Sitting	Standing	Walking	Age
1	96	93	93	26
2	85	93	70	45
3	93	90	85	22
4	90	86	89	31
5	87	98	86	24
6	87	76	74	52
7	87	93	89	27
8	84	81	86	26
Average	88.6	88.75	84	31.6

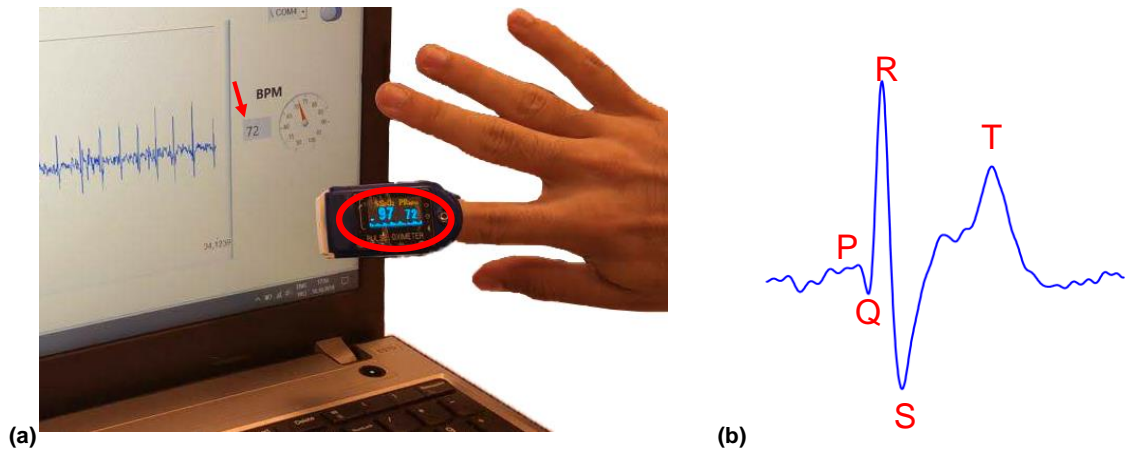


Figure 5. 4 (a) Comparison of Beat per Minute (BPM) value between clinical device and graphene textile electrode and (b) Taken ECG signal wave (P wave-QRS complex-T wave)

Table 5.2 Beat Per Minute (Bpm) Values For Eight Participants When Sitting, Standing And Walking

Subject	Sitting	Standing	Walking
1	65	72	70
2	85	92	96
3	88	99	89
4	68	80	81
5	72	110	92
6	76	96	77
7	76	88	92
8	65	76	72
Average	74.4	89.1	83.6

Combining graphene and the armband to receive heart signals promises to significantly simplify the ability to acquire, store and manipulate bio-potential data, while providing a greatly reduced maintenance cycle and improving patient comfort.

5.2. Graphene Garment

In this section, ECG signals were successfully obtained by using graphene-armband produced by stencil printing method. In addition, Ag / AgCl electrodes were placed in the same positions near the graphene coated parts of the arm band. Both electrodes were fed through the designed ecg circuit so that samples could be compared without bias. This garment was compared to the conventional pre-gelled Ag/AgCl electrode when recording ECG signals with two participants for different cases. ECG signals are taken from three different regions at the upper arm by biopotential electrodes. Separated three biopotential electrodes are placed onto the skin. We fabricated not only graphene-coated electrodes but also garment was coated graphene onto three different regions. These regions were determined as lead points according to the ECG recording signal. As a first step, these regions were covered by graphene oxide (GO). After the covering step, the chemical process was applied to make reduced graphene oxide. Reduced graphene oxide coated garment was characterized to confirm whether it can be biopotential electrodes. Characterization results were mention in chapter 4 as to garment.

We designed a wireless single arm band heart monitoring system. The ECG signals were obtained from two healthy male volunteers who were 27 and 31 years old. No skin preparation or cleaning was acted before the electrodes were placed. In order to determine the quality of the produced graphene-armband, 15-second ECG signals were taken from graphene-armband and pre-gelled Ag / AgCl electrodes in sitting, standing and walking positions. High correlation rates were obtained in the signals obtained from both subjects. By calculating the correlation values in Matlab, the reached highest correlation value was 95% by standing and the lowest correlation value was 84% by walking. Figure 5.5 shows the signals and correlation values for each case in detail

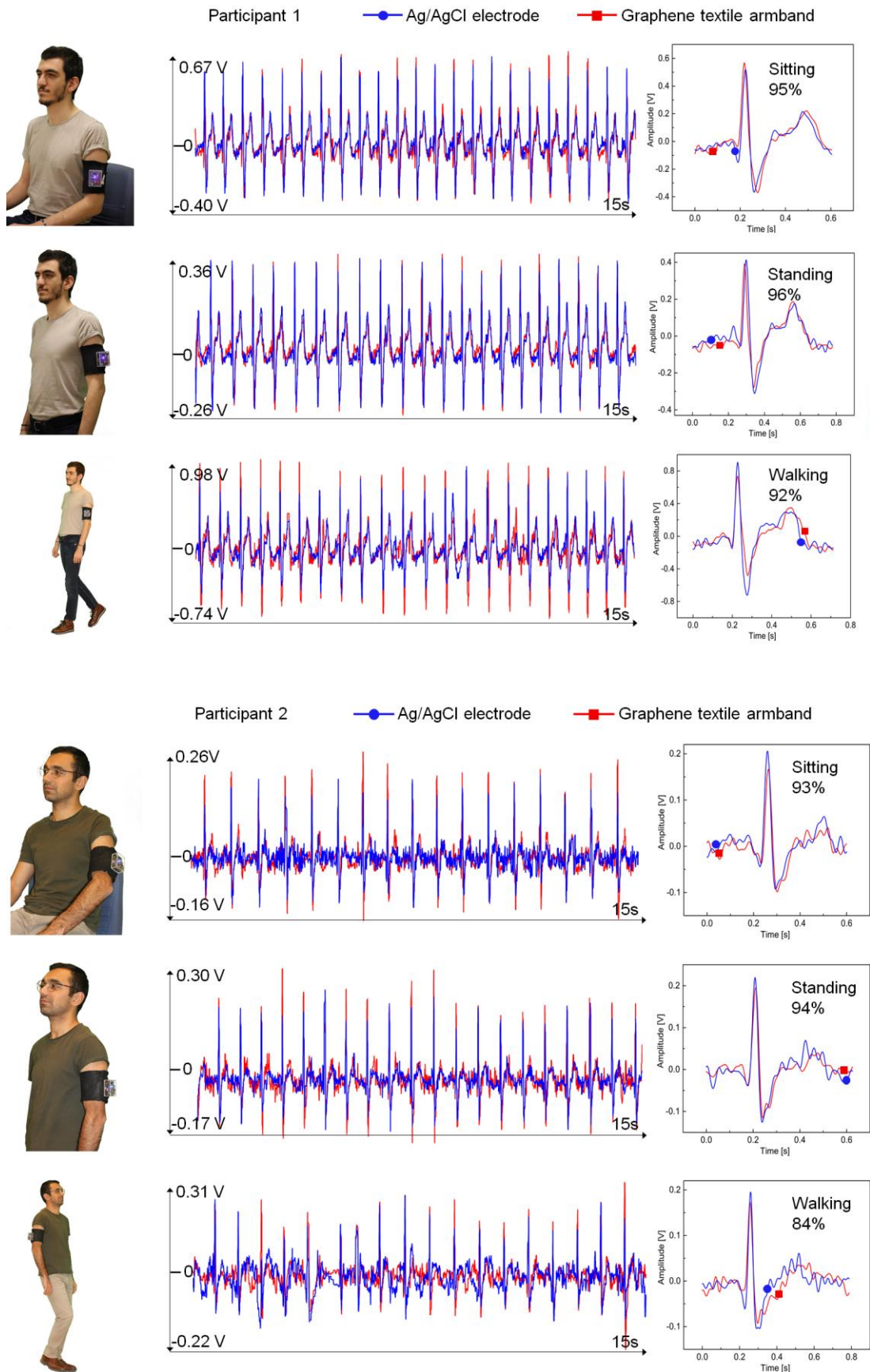


Figure 5.5 Graphs of ECG signals taken from two participants in three different positions; sitting, standing and walking and correlation values between Ag/AgCl electrodes and graphene textile armband

Except from sitting, standing, walking cases, with his arm in the air, in the 45-degree position, and in the 90 degree the ECG signal could be received as shown in figure 5.6. Since it is normally possible to interfere with the EMG signal or noise signals due to motion artifact in these situations, it is difficult to receive the ECG signal in this case. Yan be seen in the figure x, in the signals, typical ECG characteristics, QRS complex, P wave and T wave, are clearly visible. The QRS complex occurs when the ventricles in the heart depolarize. P wave occurs before the QRS complex and T wave occurs after the QRS complex [163], [164].

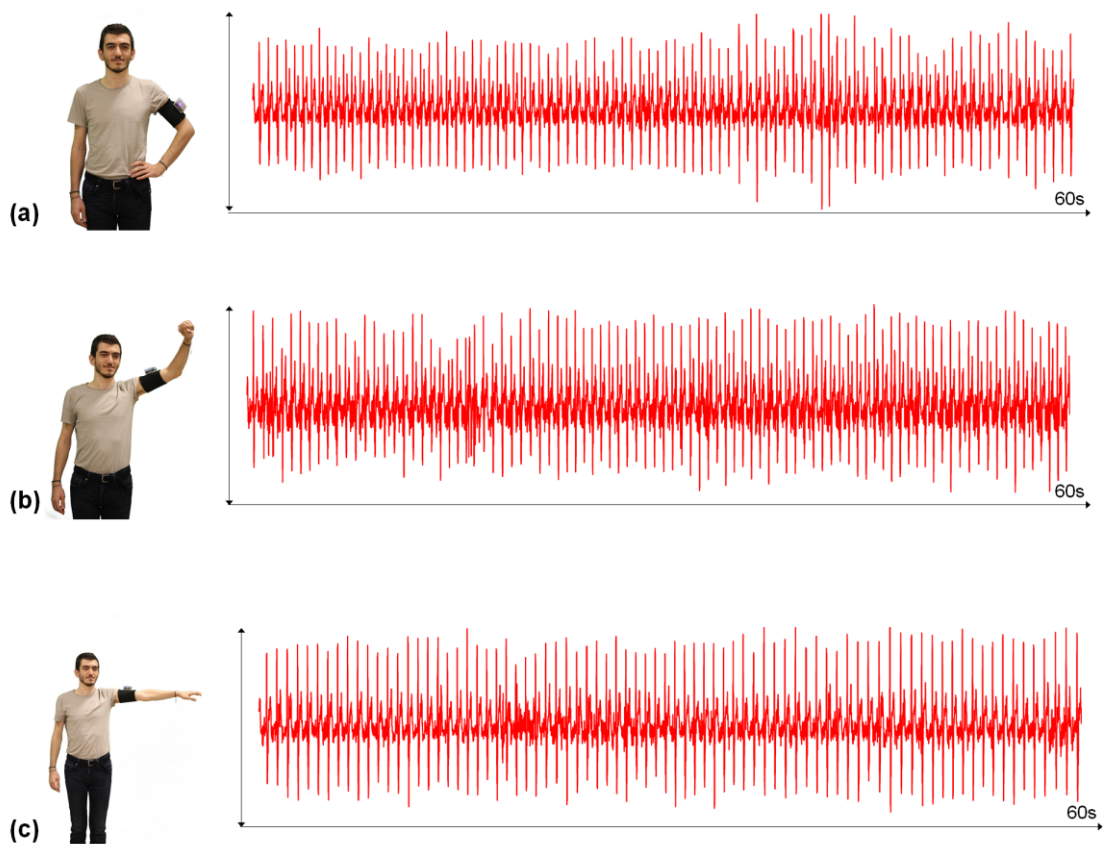


Figure 5.6 Graphs of ECG signals from his arm (a) in the air, (b) in the 180-degree position, and (c) in the 90 degree position

Taking hear rate value from the ECG monitoring system was compared to a clinical HR device. According to the obtained results, ECG signals obtained from graphene-armband produced by screen printing showed high similarity with ECG signals received from Ag / AgCl electrodes, which means that graphene armband can be shown as an alternative to

conventional electrodes and the graphene armband is more comfortable, reusable and wearable good electrode performance. It was found that the signals from the graphene armband were better and the motion artifact was less.

Signals were received in noisy environments with many instruments. The results show graphene-aramband obtained by covering three points in textile with graphene oxide and then reduced to receive bio-potential signals very competing with traditional methods as well as ECG signal from a single arm.

6. CONCLUSION AND FUTURE WORK

Nowadays efficient and continuously heart signals monitoring has become popular, owing to the increase in heart diseases and budgets allocated to this field. Alternative electrodes to commercial Ag/AgCl electrodes have great attention due to the problems of their use in the clinic applications. Moreover, they are not comfortable for patients for long term monitoring. Investments in wearable electronic clothing have increased day by day due to the many advantages of textile.

It is a challenge to produce an electrode with features such as making a real-time monitoring system both wearable and not disturbing the patient in long-term use and being continuously usable. This is because ECG signals can usually be obtained from leads on the chest or leads from limbs. At these points, it reduces the wearability of the electrodes.

In this study, we reported the system that we embedded graphene-coated textile electrodes onto a single armband that can communicate data transfer wirelessly.

Both production techniques and performance and criteria of textile-based ECG electrodes were investigated. Textile-based electrodes must be easily reproducible, reusable and uncomfortable to increase wearability. For example, in metal-coated textile electrodes, metals may irritate the body or cause discomfort after some time.

In ECG signal reception, electrode construction and construction techniques as well as the type of textile are as important as the signal acquisition system. Since produced electrodes will affect performance values such as motion artifact, skin electrode impedance, great care has been taken and characterization tests have been performed at every stage of the electrodes. While producing graphene coated electrodes, some

chemical processes and thermal treatments were applied. In addition, graphene coated electrodes which were integrated into an armband are produced by using dip-coating technique. Graphene armband was produced using stencil printing technique. The same signal acquisition system was used for electrodes produced by both techniques. Graphene garment using Stencil printing technique is easier to produce because it does not require any integrated process. It is also more useful because it is more compatible with the arm and has better contact with the skin.

ECG signals and heart rhythm rates of the nine healthy individuals, who were different age ranges were detected for three different positions, sitting, standing and walking by the system, which is formed by combining graphene coated textile electrodes with an armband successfully. The correlation rate of graphene textile electrodes with the Ag/AgCl electrodes was 98% showed that ECG waveforms performed almost the same with the commercial electrodes.

An ECG system worn into a single arm and transmits the collected data wirelessly helps maximum comfort to the user. Besides, preparation is not mandatory before signal recording as Ag/AgCl electrodes.

With Graphene garment, we successfully received ECG signals from 2 different healthy people while sitting, standing and walking. Heart rate values were also recorded when receiving the signals. Data was sent to personal computer (PC) wirelessly. When Ag / AgCl electrodes and garment graphene were compared, a high correlation value of 96 percent was obtained.

One of the biggest challenges of the arm signals is that EMG signals interfere with ECG signals. However, with the system we designed, one participant could receive ECG signals with the arm in the air, at 90 degrees, and at 180 degrees with P-QRS-T waves visible.

It has also been a promising study to make wearable ECG devices (e.g. Holter monitors), which are of great importance in the diagnosis of many conditions, from heart disease to depression. The prototype can efficiently monitor the user when physical activity and ordinary daily life.

Coupled with advances in semiconductor technology and wireless interfaces, this technology has the potential to be ubiquitous in the commercial industries. With the development of technology, the development of such devices will become significantly cheaper and attractive for everyday applications of brain-computer interfaces and monitoring devices. Future developments will be based on receiving bio-potential signals using a system of different electrode configurations.

BIBLIOGRAPHY

- [1] T. I. Oh *et al.*, “Nanofiber web textile dry electrodes for long-term biopotential recording,” *IEEE Trans. Biomed. Circuits Syst.*, vol. 7, no. 2, pp. 204–211, 2013.
- [2] Y. M. Chi, T. Jung, and G. Cauwenberghs, “Dry-Contact and Noncontact Biopotential Electrodes: Methodological Review,” *IEEE Rev. Biomed. Eng.*, vol. 3, pp. 106–119, 2010.
- [3] P. J. Xu, H. Zhang, and X. M. Tao, “Textile-structured electrodes for electrocardiogram,” *Text. Prog.*, vol. 40, no. 4, pp. 183–213, 2008.
- [4] G. Cho, K. Jeong, M. J. Paik, Y. Kwun, and M. Sung, “Performance Evaluation of Textile-Based Electrodes and Motion Sensors for Smart Clothing,” *IEEE Sens. J.*, vol. 11, no. 12, pp. 3183–3193, 2011.
- [5] N. Lacerda Silva, L. M. Gonçalves, and H. Carvalho, “Deposition of conductive materials on textile and polymeric flexible substrates,” *J. Mater. Sci. Mater. Electron.*, vol. 24, no. 2, pp. 635–643, 2013.
- [6] Y. Meng, Z. B. Li, X. Chen, and J. P. Chen, “A flexible dry micro-dome electrode for ECG monitoring,” *Microsyst. Technol.*, vol. 21, no. 6, pp. 1241–1248, 2015.
- [7] G. Paul, R. Torah, S. Beeby, and J. Tudor, “The development of screen printed conductive networks on textiles for biopotential monitoring applications,” *Sensors Actuators, A Phys.*, 2014.
- [8] L. Rattfält, F. Björefors, D. Nilsson, X. Wang, P. Norberg, and P. Ask, “Properties of screen printed electrocardiography smartware electrodes investigated in an electro-chemical cell,” *Biomed. Eng. Online*, vol. 12, no. 1, p. 64, 2013.
- [9] G. Paul, R. Torah, S. Beeby, and J. Tudor, “Novel active electrodes for ECG monitoring on woven textiles fabricated by screen and stencil printing,” *Sensors Actuators A Phys.*, vol. 221, pp. 60–66, Jan. 2015.
- [10] C. R. Merritt, H. T. Nagle, and E. Grant, “Fabric-based active electrode design and fabrication for health monitoring clothing,” *IEEE Trans. Inf. Technol.*

- Biomed.*, vol. 13, no. 2, pp. 274–280, 2009.
- [11] L. Rattfält, M. Lindén, P. Hult, L. Berglin, and P. Ask, “Electrical characteristics of conductive yarns and textile electrodes for medical applications,” *Med. Biol. Eng. Comput.*, vol. 45, no. 12, pp. 1251–1257, 2007.
- [12] V. Marozas, A. Petrenas, S. Daukantas, and A. Lukosevicius, “A comparison of conductive textile-based and silver/silver chloride gel electrodes in exercise electrocardiogram recordings,” *J. Electrocardiol.*, vol. 44, no. 2, pp. 189–194, 2011.
- [13] M. Stoppa and A. Chiolerio, “Wearable electronics and smart textiles: a critical review,” *sensors*, vol. 14, no. 7, pp. 11957–11992, 2014.
- [14] M. K. Yapici, T. Alkhidir, Y. A. Samad, and K. Liao, “Graphene-clad textile electrodes for electrocardiogram monitoring,” *Sensors Actuators B Chem.*, vol. 221, pp. 1469–1474, 2015.
- [15] M. H. Moradi, M. A. Rad, and R. B. Khezerloo, “ECG signal enhancement using adaptive Kalman filter and signal averaging,” *Int. J. Cardiol.*, vol. 173, no. 3, pp. 553–555, 2014.
- [16] T. Alkhidir, A. Sluzek, and M. K. Yapici, “Simple method for adaptive filtering of motion artifacts in E-textile wearable ECG sensors,” in *2015 37th Annual International Conference of the IEEE Engineering in Medicine and Biology Society (EMBC)*, 2015, pp. 3807–3810.
- [17] “Cardiovascular Diseases (CVDs).” .
- [18] G.-Z. Yang and G. Yang, *Body sensor networks*, vol. 1. Springer, 2006.
- [19] L. Sörnmo and P. Laguna, “The electrocardiogram—A brief background,” *Bioelectrical Signal Process. Card. Neurol. Appl. 1st ed.*; Sörnmo, L., Laguna, P., Eds, pp. 411–452, 2005.
- [20] M. Yapici and T. Alkhidir, “Intelligent medical garments with graphene-functionalized smart-cloth ECG sensors,” *Sensors*, vol. 17, no. 4, p. 875, 2017.
- [21] H. Qin, J. Li, B. He, J. Sun, L. Li, and L. Qian, “Novel wearable electrodes based on conductive chitosan fabrics and their application in smart garments,” *Materials (Basel)*, vol. 11, no. 3, p. 370, 2018.
- [22] T. Pola and J. Vanhala, “Textile electrodes in ECG measurement,” in *2007 3rd International Conference on Intelligent Sensors, Sensor Networks and Information*, 2007, pp. 635–639.
- [23] S. Jang, J. Cho, K. Jeong, and G. Cho, “Exploring possibilities of ECG electrodes

- for bio-monitoring smartwear with Cu sputtered fabrics,” in *International Conference on Human-Computer Interaction*, 2007, pp. 1130–1137.
- [24] X. An and G. Stylios, “A Hybrid Textile Electrode for Electrocardiogram (ECG) Measurement and Motion Tracking,” *Materials (Basel)*, vol. 11, no. 10, p. 1887, 2018.
- [25] M. M. Puurtinen, S. M. Komulainen, P. K. Kauppinen, J. A. V Malmivuo, and J. A. K. Hyttinen, “Measurement of noise and impedance of dry and wet textile electrodes, and textile electrodes with hydrogel,” in *2006 International Conference of the IEEE Engineering in Medicine and Biology Society*, 2006, pp. 6012–6015.
- [26] R. Pawlak, E. Korzeniewska, C. Koneczny, and B. Hałgas, “Properties of thin metal layers deposited on textile composites by using the PVD method for textronic applications,” *Autex Res. J.*, vol. 17, no. 3, pp. 229–237, 2017.
- [27] A. Ankhili, X. Tao, C. Cochrane, D. Coulon, and V. Koncar, “Washable and reliable textile electrodes embedded into underwear fabric for electrocardiography (ECG) monitoring,” *Materials (Basel)*, vol. 11, no. 2, p. 256, 2018.
- [28] G. Paul, R. Torah, S. Beeby, and J. Tudor, “The development of screen printed conductive networks on textiles for biopotential monitoring applications,” *Sensors Actuators A Phys.*, vol. 206, pp. 35–41, 2014.
- [29] N. Karim *et al.*, “All inkjet-printed graphene-based conductive patterns for wearable e-textile applications,” *J. Mater. Chem. C*, vol. 5, no. 44, pp. 11640–11648, 2017.
- [30] A. Boehm, X. Yu, W. Neu, S. Leonhardt, and D. Teichmann, “A novel 12-lead ECG T-shirt with active electrodes,” *Electronics*, vol. 5, no. 4, p. 75, 2016.
- [31] H.-J. Yoo, J. Yoo, and L. Yan, “Wireless fabric patch sensors for wearable healthcare,” in *2010 Annual International Conference of the IEEE Engineering in Medicine and Biology*, 2010, pp. 5254–5257.
- [32] M. Silva, A. Catarino, H. Carvalho, A. Rocha, J. Monteiro, and G. Montagna, “Study of vital sign monitoring with textile sensors in swimming pool environment,” in *2009 35th Annual Conference of IEEE Industrial Electronics*, 2009, pp. 4426–4431.
- [33] S. Bouwstra, W. Chen, L. Feijs, and S. B. Oetomo, “Smart jacket design for neonatal monitoring with wearable sensors,” in *2009 Sixth International*

- Workshop on Wearable and Implantable Body Sensor Networks*, 2009, pp. 162–167.
- [34] J. Coosemans, B. Hermans, and R. Puers, “Integrating wireless ECG monitoring in textiles,” *Sensors Actuators A Phys.*, vol. 130, pp. 48–53, 2006.
- [35] J. W. Zheng, Z. B. Zhang, T. H. Wu, and Y. Zhang, “A wearable mobihealth care system supporting real-time diagnosis and alarm,” *Med. Biol. Eng. Comput.*, vol. 45, no. 9, pp. 877–885, 2007.
- [36] J. Mohammed, C.-H. Lung, A. Ocneanu, A. Thakral, C. Jones, and A. Adler, “Internet of things: Remote patient monitoring using web services and cloud computing,” in *2014 IEEE International Conference on Internet of Things (iThings), and IEEE Green Computing and Communications (GreenCom) and IEEE Cyber, Physical and Social Computing (CPSCom)*, 2014, pp. 256–263.
- [37] C. R. Merritt, H. T. Nagle, and E. Grant, “Fabric-based active electrode design and fabrication for health monitoring clothing,” *IEEE Trans. Inf. Technol. Biomed.*, vol. 13, no. 2, pp. 274–280, 2009.
- [38] D. T. H. Lai, M. Palaniswami, and R. Begg, *Healthcare sensor networks: challenges toward practical implementation*. CRC Press, 2011.
- [39] G. López, V. Custodio, and J. I. Moreno, “LOBIN: E-textile and wireless-sensor-network-based platform for healthcare monitoring in future hospital environments,” *IEEE Trans. Inf. Technol. Biomed.*, vol. 14, no. 6, pp. 1446–1458, 2010.
- [40] C. E. Darling *et al.*, “Bioimpedance-Based Heart Failure Deterioration Prediction Using a Prototype Fluid Accumulation Vest-Mobile Phone Dyad: An Observational Study,” *JMIR Cardio*, vol. 1, no. 1, p. e1, 2017.
- [41] P. S. Pandian *et al.*, “Smart Vest: Wearable multi-parameter remote physiological monitoring system,” *Med. Eng. Phys.*, vol. 30, no. 4, pp. 466–477, 2008.
- [42] S. Coyle *et al.*, “BIOTEX—Biosensing textiles for personalised healthcare management,” *IEEE Trans. Inf. Technol. Biomed.*, vol. 14, no. 2, pp. 364–370, 2010.
- [43] F. Buttussi and L. Chittaro, “MOPET: A context-aware and user-adaptive wearable system for fitness training,” *Artif. Intell. Med.*, vol. 42, no. 2, pp. 153–163, 2008.
- [44] M. Di Rienzo, E. Vaini, and P. Lombardi, “Development of a smart garment for the assessment of cardiac mechanical performance and other vital signs during

- sleep in microgravity,” *Sensors Actuators A Phys.*, vol. 274, pp. 19–27, 2018.
- [45] C. Linti, H. Horter, P. Osterreicher, and H. Planck, “Sensory baby vest for the monitoring of infants,” in *International Workshop on Wearable and Implantable Body Sensor Networks (BSN’06)*, 2006, pp. 3-pp.
- [46] M. Weder *et al.*, “Embroidered electrode with silver/titanium coating for long-term ECG monitoring,” *Sensors*, vol. 15, no. 1, pp. 1750–1759, 2015.
- [47] G. Acar, O. Ozturk, and M. K. Yapici, “Wearable Graphene Nanotextile Embedded Smart Armband for Cardiac Monitoring,” *Proc. IEEE Sensors*, vol. 2018-Octob, pp. 1–4, 2018.
- [48] J. Ottenbacher, S. Romer, C. Kunze, U. Großmann, and W. Stork, “Integration of a bluetooth based ECG system into clothing,” in *Eighth International Symposium on Wearable Computers*, 2004, vol. 1, pp. 186–187.
- [49] T. Linz, C. Kallmayer, R. Aschenbrenner, and H. Reichl, “Fully untegrated EKG shirt based on embroidered electrical interconnections with conductive yarn and miniaturized flexible electronics,” in *International Workshop on Wearable and Implantable Body Sensor Networks (BSN’06)*, 2006, pp. 4-pp.
- [50] D. E. Carney and M. C. Hamrick, “Cardiovascular physiology,” *Handb. Pediatr. Surg. Patient Care*, pp. 15–25, 2013.
- [51] P. A. Iaizzo, *Handbook of cardiac anatomy, physiology, and devices*. Springer Science & Business Media, 2009.
- [52] J. Oliver, *Cardiovascular Physiology Concepts (2nd Ed.)*, vol. 53, no. 9. 2013.
- [53] S. S. Barold, “Willem Einthoven and the Birth of Clinical Electrocardiography a Hundred Years Ago,” *Card. Electrophysiol. Rev.*, vol. 7, no. 1, pp. 99–104, 2003.
- [54] “The ECG leads: electrodes, limb leads, chest (precordial) leads, 12-Lead ECG (EKG) – ECG learning,” *ECG learning*, 2019. [Online]. Available: <https://ecgwaves.com/topic/ekg-ecg-leads-electrodes-systems-limb-chest-precordial/>.
- [55] A. Macy, “The Handbook of Human Physiological Recording,” *Referenced*, vol. 7, p. 2017, 2015.
- [56] J. G. Webster, *Medical instrumentation: application and design*. John Wiley & Sons, 2009.
- [57] C. Guger, G. Krausz, B. Z. Allison, and G. Edlinger, “Comparison of dry and gel based electrodes for P300 brain–computer interfaces,” *Front. Neurosci.*, vol. 6, p. 60, 2012.

- [58] J. J. Carr and J. M. Brown, *Introduction to biomedical equipment technology*. John Wiley & Sons, 1981.
- [59] E. Huigen, “Noise characteristics of surface electrodes,” *Univ. Amsterdam, Sect. Med. Phys.*, 2001.
- [60] A. J. Golparvar and M. K. Yapici, “Wearable graphene textile-enabled EOG sensing,” in *2017 IEEE SENSORS*, 2017, pp. 1–3.
- [61] J. Muhlsteff and O. Such, “Dry electrodes for monitoring of vital signs in functional textiles,” in *The 26th Annual International Conference of the IEEE Engineering in Medicine and Biology Society*, 2004, vol. 1, pp. 2212–2215.
- [62] Y.-H. Chen *et al.*, “Soft, comfortable polymer dry electrodes for high quality ECG and EEG recording,” *Sensors*, vol. 14, no. 12, pp. 23758–23780, 2014.
- [63] K. C. Tseng, B.-S. Lin, L.-D. Liao, Y.-T. Wang, and Y.-L. Wang, “Development of a wearable mobile electrocardiogram monitoring system by using novel dry foam electrodes,” *IEEE Syst. J.*, vol. 8, no. 3, pp. 900–906, 2013.
- [64] C.-T. Lin, L.-D. Liao, Y.-H. Liu, I.-J. Wang, B.-S. Lin, and J.-Y. Chang, “Novel dry polymer foam electrodes for long-term EEG measurement,” *IEEE Trans. Biomed. Eng.*, vol. 58, no. 5, pp. 1200–1207, 2010.
- [65] A. Gruetzmann, S. Hansen, and J. Müller, “Novel dry electrodes for ECG monitoring,” *Physiol. Meas.*, vol. 28, no. 11, p. 1375, 2007.
- [66] P. Griss, H. K. Tolvanen-Laakso, P. Merilainen, and G. Stemme, “Characterization of micromachined spiked biopotential electrodes,” *IEEE Trans. Biomed. Eng.*, vol. 49, no. 6, pp. 597–604, 2002.
- [67] W. Zhou *et al.*, “Fabrication and impedance measurement of novel metal dry bioelectrode,” *Sensors Actuators A Phys.*, vol. 201, pp. 127–133, 2013.
- [68] C.-Y. Chen, C.-L. Chang, T.-F. Chien, and C.-H. Luo, “Flexible PDMS electrode for one-point wearable wireless bio-potential acquisition,” *Sensors Actuators A Phys.*, vol. 203, pp. 20–28, 2013.
- [69] H.-C. Jung *et al.*, “CNT/PDMS composite flexible dry electrodes for long-term ECG monitoring,” *IEEE Trans. Biomed. Eng.*, vol. 59, no. 5, pp. 1472–1479, 2012.
- [70] P. Griss, P. Enoksson, H. Tolvanen-Laakso, P. Merilainen, S. Ollmar, and G. Stemme, “Spiked biopotential electrodes,” in *Proceedings IEEE Thirteenth Annual International Conference on Micro Electro Mechanical Systems (Cat. No. 00CH36308)*, 2000, pp. 323–328.

- [71] C. W. Chang and J. C. Chiou, "Surface-mounted dry electrode and analog-front-end systems for physiological signal measurements," in *2009 IEEE/NIH Life Science Systems and Applications Workshop*, 2009, pp. 108–111.
- [72] A. Searle and L. Kirkup, "A direct comparison of wet, dry and insulating bioelectric recording electrodes," *Physiol. Meas.*, vol. 21, no. 2, p. 271, 2000.
- [73] D. Mazouzi *et al.*, "Critical roles of binders and formulation at multiscales of silicon-based composite electrodes," *J. Power Sources*, vol. 280, pp. 533–549, 2015.
- [74] B. Taji, S. Shirmohammadi, V. Groza, and I. Batkin, "Impact of skin–electrode interface on electrocardiogram measurements using conductive textile electrodes," *IEEE Trans. Instrum. Meas.*, vol. 63, no. 6, pp. 1412–1422, 2013.
- [75] L. Beckmann *et al.*, "Characterization of textile electrodes and conductors using standardized measurement setups," *Physiol. Meas.*, vol. 31, no. 2, p. 233, 2010.
- [76] H. Gong, "Fancy yarns," in *Textile and Clothing Design Technology*, CRC Press, 2017, pp. 87–107.
- [77] A. Baba and M. J. Burke, "Electrical characterisation of dry electrodes for ECG recording," in *WSEAS International Conference. Proceedings. Mathematics and Computers in Science and Engineering*, 2008, no. 12.
- [78] E. P. Scilingo, A. Gemignani, R. Paradiso, N. Taccini, B. Ghelarducci, and D. De Rossi, "Performance evaluation of sensing fabrics for monitoring physiological and biomechanical variables," *IEEE Trans. Inf. Technol. Biomed.*, vol. 9, no. 3, pp. 345–352, 2005.
- [79] W. Wu, S. Pirbhulal, A. K. Sangaiah, S. C. Mukhopadhyay, and G. Li, "Optimization of signal quality over comfortability of textile electrodes for ECG monitoring in fog computing based medical applications," *Futur. Gener. Comput. Syst.*, vol. 86, pp. 515–526, 2018.
- [80] A. B. Simakov and J. G. Webster, "Motion artifact from electrodes and cables," 2010.
- [81] G. Priniotakis, P. Westbroek, L. Van Langenhove, and C. Hertleer, "Electrochemical impedance spectroscopy as an objective method for characterization of textile electrodes," *Trans. Inst. Meas. Control*, vol. 29, no. 3–4, pp. 271–281, 2007.
- [82] J. G. Webster, "Reducing motion artifacts and interference in biopotential recording," *IEEE Trans. Biomed. Eng.*, no. 12, pp. 823–826, 1984.

- [83] A. Cömert and J. Hyttinen, “Investigating the possible effect of electrode support structure on motion artifact in wearable bioelectric signal monitoring,” *Biomed. Eng. Online*, vol. 14, no. 1, p. 44, 2015.
- [84] A. G. Ratz, “Triboelectric noise (Triboelectric noise in mechanically flexed low level signal cables for piezoelectric transducers with high gain amplifiers),” *ISA Trans.*, vol. 9, no. 2, pp. 154–158, 1969.
- [85] N. Meziane, S. Yang, M. Shokouejad, J. G. Webster, M. Attari, and H. Eren, “Simultaneous comparison of 1 gel with 4 dry electrode types for electrocardiography,” *Physiol. Meas.*, vol. 36, no. 3, p. 513, 2015.
- [86] B. Tajji, S. Shirmohammadi, and V. Groza, “Measuring skin-electrode impedance variation of conductive textile electrodes under pressure,” in *2014 IEEE International Instrumentation and Measurement Technology Conference (I2MTC) Proceedings*, 2014, pp. 1083–1088.
- [87] I. S. O. ISO, “6330: 2012 Textiles—Domestic Washing and Drying Procedures for Textile Testing,” *ISO Geneva, Switz.*, 2012.
- [88] D. Hegemann, M. Amberg, A. Ritter, and M. Heuberger, “Recent developments in Ag metallised textiles using plasma sputtering,” *Mater. Technol.*, vol. 24, no. 1, pp. 41–45, 2009.
- [89] J. Cho, J. Moon, K. Jeong, and G. Cho, “Application of PU-sealing into Cu/Ni electroless plated polyester fabrics for e-textiles,” *Fibers Polym.*, vol. 8, no. 3, pp. 330–334, 2007.
- [90] Y. Guo *et al.*, “PEDOT: PSS ‘wires’ printed on textile for wearable electronics,” *ACS Appl. Mater. Interfaces*, vol. 8, no. 40, pp. 26998–27005, 2016.
- [91] I. Kazani, C. Hertleer, G. De Mey, A. Schwarz, G. Guxho, and L. Van Langenhove, “Electrical conductive textiles obtained by screen printing,” *Fibres Text. East. Eur.*, vol. 20, no. 1, pp. 57–63, 2012.
- [92] S. H. Lee, S. M. Jung, C. K. Lee, K. S. Jeong, G. Cho, and S. K. Yoo, “Wearable ECG monitoring system using conductive fabrics and active electrodes,” in *International Conference on Human-Computer Interaction*, 2009, pp. 778–783.
- [93] A. Alzaidi, L. Zhang, and H. Bajwa, “Smart textiles based wireless ECG system,” in *2012 IEEE Long Island Systems, Applications and Technology Conference (LISAT)*, 2012, pp. 1–5.
- [94] Y. Zhou, X. Ding, J. Zhang, Y. Duan, J. Hu, and X. Yang, “Fabrication of conductive fabric as textile electrode for ECG monitoring,” *Fibers Polym.*, vol.

- 15, no. 11, pp. 2260–2264, 2014.
- [95] S. Takamatsu, T. Lonjaret, D. Crisp, J.-M. Badier, G. G. Malliaras, and E. Ismailova, “Direct patterning of organic conductors on knitted textiles for long-term electrocardiography,” *Sci. Rep.*, vol. 5, p. 15003, 2015.
- [96] S. Lee, Y. Lee, J. Park, and D. Choi, “Stitchable organic photovoltaic cells with textile electrodes,” *Nano Energy*, vol. 9, pp. 88–93, 2014.
- [97] I. G. Trindade, F. Martins, and P. Baptista, “High electrical conductance poly (3, 4-ethylenedioxythiophene) coatings on textile for electrocardiogram monitoring,” *Synth. Met.*, vol. 210, pp. 179–185, 2015.
- [98] M. A. Mestrovic, R. J. N. Helmer, L. Kyrtziz, and D. Kumar, “Preliminary study of dry knitted fabric electrodes for physiological monitoring,” in *2007 3rd International Conference on Intelligent Sensors, Sensor Networks and Information*, 2007, pp. 601–606.
- [99] P. J. Xu, H. Zhang, and X. M. Tao, “Textile-structured electrodes for electrocardiogram,” *Text. Prog.*, vol. 40, no. 4, pp. 183–213, 2008.
- [100] L. Xie, G. Yang, L. Xu, F. Seoane, Q. Chen, and L. Zheng, “Characterization of dry biopotential electrodes,” in *2013 35th Annual International Conference of the IEEE Engineering in Medicine and Biology Society (EMBC)*, 2013, pp. 1478–1481.
- [101] H. Zhang, W. Li, X. Tao, P. Xu, and H. Liu, “Textile-structured human body surface biopotential signal acquisition electrode,” in *2011 4th International Congress on Image and Signal Processing*, 2011, vol. 5, pp. 2792–2797.
- [102] T. Apiwattanadej, L. Zhang, and H. Li, “Electrospun polyurethane microfiber membrane on conductive textile for water-supported textile electrode in continuous ECG monitoring application,” in *2018 Symposium on Design, Test, Integration & Packaging of MEMS and MOEMS (DTIP)*, 2018, pp. 1–5.
- [103] C. Poggio, F. Trovati, M. Ceci, M. Chiesa, M. Colombo, and G. Pietrocola, “Biological and antibacterial properties of a new silver fiber post: in vitro evaluation,” *J. Clin. Exp. Dent.*, vol. 9, no. 3, p. e387, 2017.
- [104] J. C. Marquez, F. Seoane, E. Välimäki, and K. Lindecrantz, “Comparison of dry-textile electrodes for electrical bioimpedance spectroscopy measurements,” in *Journal of Physics: Conference Series*, 2010, vol. 224, no. 1, p. 12140.
- [105] M. Ishijima, “Cardiopulmonary monitoring by textile electrodes without subject-awareness of being monitored,” *Med. Biol. Eng. Comput.*, vol. 35, no. 6, pp. 685–

690, 1997.

- [106] M. Catrysse, R. Puers, C. Hertleer, L. Van Langenhove, H. Van Egmond, and D. Matthys, "Towards the integration of textile sensors in a wireless monitoring suit," *Sensors Actuators A Phys.*, vol. 114, no. 2–3, pp. 302–311, 2004.
- [107] A. Ali *et al.*, "Electrical conductivity and physiological comfort of silver coated cotton fabrics," *J. Text. Inst.*, vol. 109, no. 5, pp. 620–628, 2018.
- [108] A. M. Grancarić *et al.*, "Conductive polymers for smart textile applications," *J. Ind. Text.*, vol. 48, no. 3, pp. 612–642, 2018.
- [109] J. Jianming, P. Wei, Y. Shenglin, and L. Guang, "Electrically conductive PANI-DBSA/Co-PAN composite fibers prepared by wet spinning," *Synth. Met.*, vol. 149, no. 2–3, pp. 181–186, 2005.
- [110] J. Foroughi, G. M. Spinks, G. G. Wallace, and P. G. Whitten, "Production of polypyrrole fibres by wet spinning," *Synth. Met.*, vol. 158, no. 3–4, pp. 104–107, 2008.
- [111] H. Okuzaki, Y. Harashina, and H. Yan, "Highly conductive PEDOT/PSS microfibers fabricated by wet-spinning and dip-treatment in ethylene glycol," *Eur. Polym. J.*, vol. 45, no. 1, pp. 256–261, 2009.
- [112] M. Afshari, *Electrospun nanofibers*. Woodhead Publishing, 2016.
- [113] Z.-M. Huang, Y.-Z. Zhang, M. Kotaki, and S. Ramakrishna, "A review on polymer nanofibers by electrospinning and their applications in nanocomposites," *Compos. Sci. Technol.*, vol. 63, no. 15, pp. 2223–2253, 2003.
- [114] N. Bhardwaj and S. C. Kundu, "Electrospinning: a fascinating fiber fabrication technique," *Biotechnol. Adv.*, vol. 28, no. 3, pp. 325–347, 2010.
- [115] Y. Ding, W. Xu, W. Wang, H. Fong, and Z. Zhu, "Scalable and Facile Preparation of Highly Stretchable Electrospun PEDOT: PSS@ PU Fibrous Nonwovens toward Wearable Conductive Textile Applications," *ACS Appl. Mater. Interfaces*, vol. 9, no. 35, pp. 30014–30023, 2017.
- [116] G. O. Mallory and J. B. Hajdu, *Electroless plating: fundamentals and applications*. William Andrew, 1990.
- [117] J. Cho, J. Moon, K. Jeong, and G. Cho, "An exploration of electrolessly Cu/Ni plated polyester fabrics as E-textiles," in *Ninth IEEE International Symposium on Wearable Computers (ISWC'05)*, 2005, pp. 206–207.
- [118] J.-H. Jeon, S.-W. Yeom, and I.-K. Oh, "Fabrication and actuation of ionic polymer metal composites patterned by combining electroplating with electroless

- plating,” *Compos. Part A Appl. Sci. Manuf.*, vol. 39, no. 4, pp. 588–596, 2008.
- [119] D. M. Mattox, *Handbook of physical vapor deposition (PVD) processing*. William Andrew, 2010.
- [120] N. L. Silva, L. M. Gonçalves, and H. Carvalho, “Deposition of conductive materials on textile and polymeric flexible substrates,” *J. Mater. Sci. Mater. Electron.*, vol. 24, no. 2, pp. 635–643, 2013.
- [121] M. Keller, A. Ritter, P. Reimann, V. Thommen, A. Fischer, and D. Hegemann, “Comparative study of plasma-induced and wet-chemical cleaning of synthetic fibers,” *Surf. Coatings Technol.*, vol. 200, no. 1–4, pp. 1045–1050, 2005.
- [122] S. M. Shang and W. Zeng, “Conductive nanofibres and nanocoatings for smart textiles,” in *Multidisciplinary Know-How for Smart-Textiles Developers*, Elsevier, 2013, pp. 92–128.
- [123] X. Tang and X. Yan, “Dip-coating for fibrous materials: mechanism, methods and applications,” *J. Sol-Gel Sci. Technol.*, vol. 81, no. 2, pp. 378–404, 2017.
- [124] Y. Zhao, Y. Cao, J. Liu, Z. Zhan, X. Li, and W. Li, “Single-Wall Carbon Nanotube-Coated Cotton Yarn for Electrocardiography Transmission,” *Micromachines*, vol. 9, no. 3, p. 132, 2018.
- [125] A. K. Sen, *Coated textiles: principles and applications*. Crc Press, 2007.
- [126] E. Garcia-Brejjo, G. Prats-Boluda, J. V. Lidon-Roger, Y. Ye-Lin, and J. Garcia-Casado, “A comparative analysis of printing techniques by using an active concentric ring electrode for bioelectrical recording,” *Microelectron. Int.*, vol. 32, no. 2, pp. 103–107, 2015.
- [127] K. S. Novoselov, V. I. Fal, L. Colombo, P. R. Gellert, M. G. Schwab, and K. Kim, “A roadmap for graphene,” *Nature*, vol. 490, no. 7419, pp. 192–200, 2012.
- [128] J. Molina, “Graphene-based fabrics and their applications: a review,” *RSC Adv.*, vol. 6, no. 72, pp. 68261–68291, 2016.
- [129] Y.-Z. Wu, J.-X. Sun, L.-F. Li, Y.-S. Ding, and H.-A. Xu, “Performance evaluation of a novel cloth electrode,” in *2010 4th International Conference on Bioinformatics and Biomedical Engineering*, 2010, pp. 1–5.
- [130] C. L. Lam, N. N. Z. M. Rajdi, and D. H. B. Wicaksono, “MWCNT/Cotton-based flexible electrode for electrocardiography,” in *SENSORS, 2013 IEEE*, 2013, pp. 1–4.
- [131] S. Y. Madani, A. Mandel, and A. M. Seifalian, “A concise review of carbon nanotube’s toxicology,” *Nano Rev.*, vol. 4, no. 1, p. 21521, 2013.

- [132] M. Pelin *et al.*, “Differential cytotoxic effects of graphene and graphene oxide on skin keratinocytes,” *Sci. Rep.*, vol. 7, p. 40572, 2017.
- [133] H. Ujiie, *Digital printing of textiles*. Woodhead Publishing, 2006.
- [134] J. P. Hart and S. A. Wring, “Screen-printed voltammetric and amperometric electrochemical sensors for decentralized testing,” *Electroanalysis*, vol. 6, no. 8, pp. 617–624, 1994.
- [135] B. Hu *et al.*, “Textile-Based Flexible Electroluminescent Devices,” *Adv. Funct. Mater.*, vol. 21, no. 2, pp. 305–311, 2011.
- [136] B. Karaguzel *et al.*, “Utility of nonwovens in the production of integrated electrical circuits via printing conductive inks,” *J. Text. Inst.*, vol. 99, no. 1, pp. 37–45, 2008.
- [137] A. Kamyshny, J. Steinke, and S. Magdassi, “Metal-based inkjet inks for printed electronics,” *Open Appl. Phys. J.*, vol. 4, no. 1, 2011.
- [138] E. Bihar *et al.*, “Fully printed electrodes on stretchable textiles for long-term electrophysiology,” *Adv. Mater. Technol.*, vol. 2, no. 4, p. 1600251, 2017.
- [139] S.-P. Chen, H.-L. Chiu, P.-H. Wang, and Y.-C. Liao, “Inkjet printed conductive tracks for printed electronics,” *ECS J. Solid State Sci. Technol.*, vol. 4, no. 4, pp. P3026–P3033, 2015.
- [140] E. Skrzetuska, M. Puchalski, and I. Krucińska, “Chemically driven printed textile sensors based on graphene and carbon nanotubes,” *Sensors*, vol. 14, no. 9, pp. 16816–16828, 2014.
- [141] L. Allison, S. Hoxie, and T. L. Andrew, “Towards seamlessly-integrated textile electronics: methods to coat fabrics and fibers with conducting polymers for electronic applications,” *Chem. Commun.*, vol. 53, no. 53, pp. 7182–7193, 2017.
- [142] M. S. Kim *et al.*, “PET fabric/polypyrrole composite with high electrical conductivity for EMI shielding,” *Synth. Met.*, vol. 126, no. 2–3, pp. 233–239, 2002.
- [143] J. C. Slonczewski and P. R. Weiss, “Band structure of graphite,” *Phys. Rev.*, vol. 109, no. 2, p. 272, 1958.
- [144] X. Li, X. Wang, L. Zhang, S. Lee, and H. Dai, “Chemically derived, ultrasoft graphene nanoribbon semiconductors,” *Science (80-.)*, vol. 319, no. 5867, pp. 1229–1232, 2008.
- [145] J. Wu, H. A. Becerril, Z. Bao, Z. Liu, Y. Chen, and P. Peumans, “Organic solar cells with solution-processed graphene transparent electrodes,” *Appl. Phys. Lett.*,

- vol. 92, no. 26, p. 237, 2008.
- [146] V. C. Tung, M. J. Allen, Y. Yang, and R. B. Kaner, “High-throughput solution processing of large-scale graphene,” *Nat. Nanotechnol.*, vol. 4, no. 1, p. 25, 2009.
- [147] F. Schedin *et al.*, “Detection of individual gas molecules adsorbed on graphene,” *Nat. Mater.*, vol. 6, no. 9, p. 652, 2007.
- [148] E. Yoo, J. Kim, E. Hosono, H. Zhou, T. Kudo, and I. Honma, “Large reversible Li storage of graphene nanosheet families for use in rechargeable lithium ion batteries,” *Nano Lett.*, vol. 8, no. 8, pp. 2277–2282, 2008.
- [149] F. Bonaccorso, A. Lombardo, T. Hasan, Z. Sun, L. Colombo, and A. C. Ferrari, “Production and processing of graphene and 2d crystals,” *Mater. Today*, vol. 15, no. 12, pp. 564–589, 2012.
- [150] S. Park, J. An, J. R. Potts, A. Velamakanni, S. Murali, and R. S. Ruoff, “Hydrazine-reduction of graphite-and graphene oxide,” *Carbon N. Y.*, vol. 49, no. 9, pp. 3019–3023, 2011.
- [151] I. K. Moon, J. Lee, R. S. Ruoff, and H. Lee, “Reduced graphene oxide by chemical graphitization,” *Nat. Commun.*, vol. 1, p. 73, 2010.
- [152] J. Phiri, P. Gane, and T. C. Maloney, “General overview of graphene: Production, properties and application in polymer composites,” *Mater. Sci. Eng. B*, vol. 215, pp. 9–28, 2017.
- [153] L. I. Şanlı, V. Bayram, B. Yarar, S. Ghobadi, and S. A. Gürsel, “Development of graphene supported platinum nanoparticles for polymer electrolyte membrane fuel cells: Effect of support type and impregnation–reduction methods,” *Int. J. Hydrogen Energy*, vol. 41, no. 5, pp. 3414–3427, 2016.
- [154] L. Gubler, S. A. Gürsel, A. Wokaun, and G. G. Scherer, “Cross-linker effect in ETFE-based radiation-grafted proton-conducting membranes I. Properties and fuel cell performance characteristics,” *J. Electrochem. Soc.*, vol. 155, no. 9, pp. B921–B928, 2008.
- [155] B. S. Okan, A. Yürüm, N. Gorgülü, S. A. Gürsel, and Y. Yürüm, “Polypyrrole coated thermally exfoliated graphite nanoplatelets and the effect of oxygen surface groups on the interaction of platinum catalysts with graphene-based nanocomposites,” *Ind. Eng. Chem. Res.*, vol. 50, no. 22, pp. 12562–12571, 2011.
- [156] R. Y. Azeemi, R. Ergün, A. Taşdemir, S. A. Gürsel, and A. Yürüm, “A simple spray assisted method to fabricate high performance layered graphene/silicon hybrid anodes for lithium-ion batteries,” *Int. J. Hydrogen Energy*, 2019.

- [157] A. A. Iskandar, R. Kolla, K. Schilling, and W. Voelker, "A wearable 1-lead necklace ECG for continuous heart rate monitoring," in *2016 IEEE 18th International Conference on e-Health Networking, Applications and Services (Healthcom)*, 2016, pp. 1–4.
- [158] H.-C. Yang, T.-F. Chien, S.-H. Liu, and H.-H. Chiang, "Study of Single-Arm Electrode for ECG Measurement Using Flexible Print Circuit," *Dep. Electr. Eng. South. Taiwan Univ.*, 2011.
- [159] 2012. Application note # 291491: Single arm ECG measurement using EPIC, "No Title."
- [160] M. S. Spach, R. C. Barr, J. W. Havstad, and E. C. Long, "Skin-electrode impedance and its effect on recording cardiac potentials," *Circulation*, vol. 34, no. 4, pp. 649–656, 1966.
- [161] G. E. Bergey, R. D. Squires, and W. C. Sipple, "Electrocardiogram recording with pasteless electrodes," *IEEE Trans. Biomed. Eng.*, no. 3, pp. 206–211, 1971.
- [162] S. Grimnes, "Impedance measurement of individual skin surface electrodes," *Med. Biol. Eng. Comput.*, vol. 21, no. 6, pp. 750–755, 1983.
- [163] R. Gupta, M. Mitra, and J. Bera, *ECG acquisition and automated remote processing*, vol. 20. Springer, 2014.
- [164] A. Portelli and S. Nasuto, "Design and development of non-contact bio-potential electrodes for pervasive health monitoring applications," *Biosensors*, vol. 7, no. 1, p. 2, 2017.